Lawrence Berkeley Laboratory
UNIVERSITY OF CALIFORNIA

Materials & Molecular Research Division

OPTICAL PROPERTIES OF MOLECULES CHEMISORBED ON THE Ni(111) SURFACE

C.B. Harris, H.J. Robota, and P.M. Whitmore

February 1981
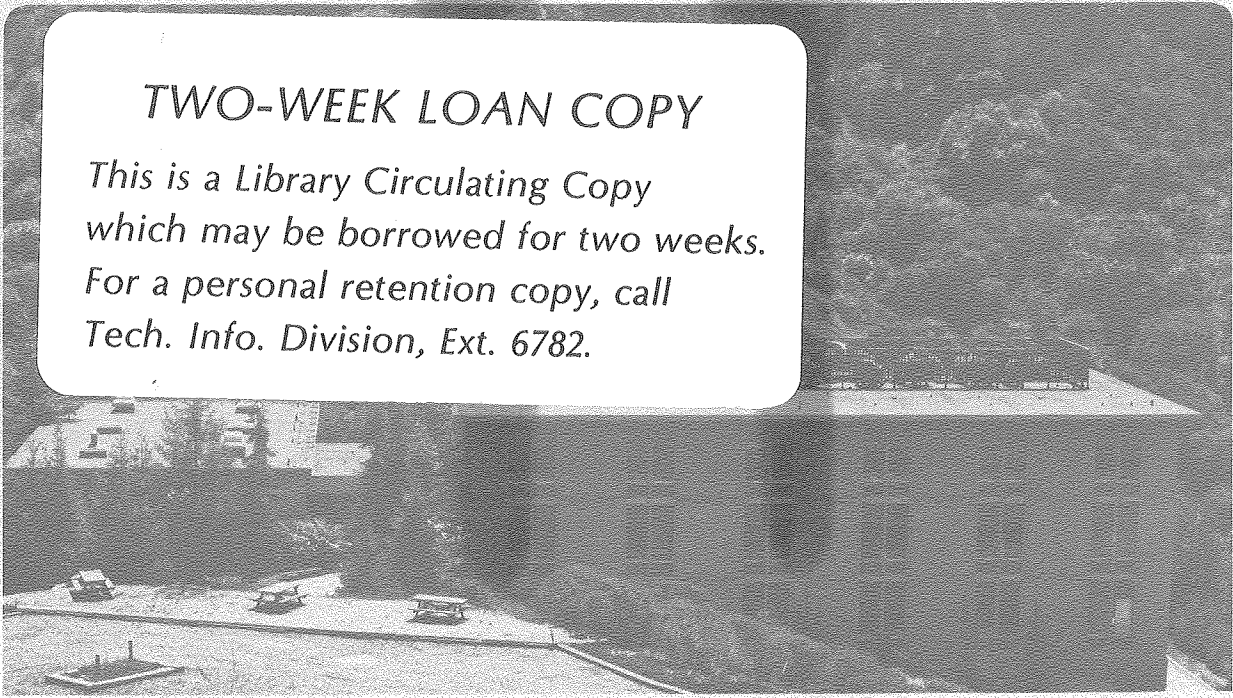
DISCLAIMER

This document was prepared as an account of work sponsored by the United States Government. While this document is believed to contain correct information, neither the United States Government nor any agency thereof, nor the Regents of the University of California, nor any of their employees, makes any warranty, express or implied, or assumes any legal responsibility for the accuracy, completeness, or usefulness of any information, apparatus, product, or process disclosed, or represents that its use would not infringe privately owned rights. Reference herein to any specific commercial product, process, or service by its trade name, trademark, manufacturer, or otherwise, does not necessarily constitute or imply its endorsement, recommendation, or favoring by the United States Government or any agency thereof, or the Regents of the University of California. The views and opinions of authors expressed herein do not necessarily state or reflect those of the United States Government or any agency thereof or the Regents of the University of California.

Optical Properties of Molecules Chemisorbed on the Ni(111) Surface.

C. B. Harris, H. J. Robota and P. M. Whitmore

Department of Chemistry and Materials and Molecular Research Division of
Lawrence Berkeley Laboratory, University of California
Berkeley, California 94720

ABSTRACT

The adsorption of a variety of molecules on Ni(111) is studied by
UV/visible spectroscopic ellipsometry. The spectra were analyzed within
a simple dielectric model. The absorption spectra of annealed, thin,
condensed layers of pyrazine, pyridine, and naphthalene on the Ni(111)
surface resemble bulk crystal spectra, indicating minimal perturbations
due to the metal substrate. Chemisorption of molecules on the Ni(111)
surface produced enhanced absorption between 2800Å and 3100Å. The wide
range of adsorbate properties and surface chemistry suggest a modification
of the optical response of the metal upon chemisorption. This enhanced
optical absorption is attributed to nonvertical interband transitions
made possible by loss of translational invariance at the surface.

This manuscript was printed from originals provided by the authors.

I. INTRODUCTION

Significant improvement in calculation techniques and experimental expertise has led to a greater understanding of the properties of atoms and molecules bound to metal surfaces. Knowledge of the type of bonding, energies of occupied orbitals, and the geometrical arrangement of adsorbed species represents the aggregate of information available from a host of surface experimental probes. However, a detailed understanding of the roles played by both adsorbate and substrate in the formation of surface bonds remains unavailable from present methods. Further, the nature of electronically excited states of the adsorbate-substrate system may be only inferred from subtle variations in the results of direct probes. The use of spectroscopic absorption and emission experiments provides significant information concerning the properties of electronically excited atoms and molecules in many other types of environment. These methods have led to a general understanding of complex chemical reaction dynamics. It is hoped that similar progress can be made in understanding the chemistry and catalytic behavior of many metal surfaces.

Unlike the plethora of experimental reports and theoretical contributions available for most surface probes, only very few reports of spectroscopic absorption investigations for species adsorbed on metal surfaces have been published[1-9]. Undoubtedly, the extreme difficulty in performing such experiments reliably and the difficult task of interpreting the results within the framework of present knowledge stand as the reasons for such inactivity. Perhaps the most successful results have been reported by Restorff and Drew[4] who used surface reflectance spectroscopy to study the chemisorption of H_2 on the (100), (110) and (111) surfaces of tungsten. The chemisorption-induced optical

absorption of the hydrogen atoms was effectively interpreted with the aid

of a surface band structure calculation. Further, the appearance of "negative

strength" oscillators believed due to the loss of intrinsic metal surface

states provided information about the restructuring of the substrate electronic

properties. Although not performed on single crystal samples, the work of

Moskovits and McBreen[8] using a polarization modulation method concerning

a variety of gases on evaporated copper films also provides evidence both

for absorption processes within the chemisorbed complex and the influence

of the metal substrate in producing spectral features. The interesting inter-

pretation of results for submonolayer films of rare gases on a number of

substrates is also of note[6,7]. While not a detailed account of the several

absorption investigations, this group of results demonstrates the range of

problems that can be investigated using available techniques.

It is the purpose of this report to relate the results of spectroscopic

studies of various gases chemisorbed on the nickel (111) surface in a well-

characterized environment. The results were obtained and interpreted within

the framework of ellipsometric methods which are described in greater detail

in the experimental section. As an introduction to these experiments, it is

useful to discuss briefly the possible types of behavior one might expect

for systems of molecules adsorbed on single crystal metal surfaces[10].

The effects can be roughly divided into three basic types: (1) minor modifi-

cation of adsorbate states leading to new"molecular" -type optical absorptions;

(2) interaction of nominally distinct adsorbate and metal states to produce

charge transfer or ionic complex transitions; (3) changes in the optical response

of the metallic substrate induced by adsorption.

Absorption spectra of overlayers which interact only weakly with the

metal are expected to reflect slightly modified molecular transitions. In

fact, spectra of condensed pyrazine on nickel (111) have been previously reported[9], and the transition energies and vibronic spacings observed are very close to those in molecular crystal studies of pyrazine. As the interaction between adsorbate and metal increases, the possibility arises for new features in the optical spectrum. Shifts in peak energies, vibronic spacings, and excited state lifetimes are likely because of the strong influence of the metal surface. Forbidden transitions in the free adsorbate molecules could become allowed through the spin-orbit mediation of the metal centers. Recent UPS studies have clearly demonstrated that many adsorbed molecules retain much of their molecular character upon chemisorption, and it is only those molecular orbitals which are directly involved in bond formation which are significantly altered[11]. This observation makes the prospect for obtaining information from spectra of chemisorbed molecules most attractive. If spectral features of chemisorbed overlayers can be correlated to free molecule electronic configurations, then, in principle, the molecular orbitals involved in bond formation can be identified and the role of unoccupied molecular orbitals and molecular excited states in surface bonding can be assessed. This information is presently unavailable from existing surface sensitive techniques.

As the strength of the interaction between adsorbate and metal increases, it becomes more likely that features in the overlayer spectrum will not be easily related to the free molecule. For example, charge transfer excitations from metal to ligand or vice versa are common in the spectra of organometallic complexes, and some studies of chemisorbed systems have assigned some broad absorption peaks to such charge transfer bands[5, 12]. In the extreme case of ionic chemisorptive bonding, where electron transfer is complete in the ground state complex, the absorption spectrum may resemble that of the molecular

anion or cation, depending on the direction of electron transfer.

Finally, the features observed in the analyzed spectrum could in fact arise from changes in the optical response of the metal surface. Separation of optical response of the surface from that of the bulk is difficult, but several adsorption-induced effects on the metal spectrum can be qualitatively visualized. An obvious effect of adsorbing a layer of gas on the metal surface is a change in the dielectric function at the boundary of the metal. The effect on the optical spectrum would be most pronounced in the wavelength region where collective oscillations, e. g., surface plasmons, can occur. A shift in plasmon energy or enhancement could be expected. Strong interaction of the adsorbate with the metal could produce or remove surface resonances or surface states, as well as change the contribution of non-local, or wave-vector dependent, effects to the total dielectric function of the metal. Of particular interest in regions where interband transitions are possible, the adsorption of gases may affect the spectrum by altering the potential and the symmetry at the surface and thus the response of the bulk electrons either normal to or parallel to the surface.

The molecule chosen for initial investigation was pyrazine (1,4 diazabenzene). The spectrum of pyrazine condensed on nickel (111) has been studied previously[9] and exhibits two strong absorption bands, an $n\pi^*$ transition at 3327Å and $\pi\pi^*$ at 2670Å. Each band has vibronic progressions which, along with the transition energies, indicate a molecular environment mildly perturbed from that in the pyrazine crystal[13]. These strong features with sharp vibronic structure made the prospect of detecting and studying the chemisorbed species good. In addition to the chances for success, the chemisorption of pyrazine

is interesting in itself because of the possibility of two types of bonding, through the nitrogen lone pairs or through the ring π system. Pyridine also is of interest for the same reason, and, since it also has strong molecular transitions[14] in our accessible wavelength region, it was also studied. Naphthalene was later chosen because it has strong optical absorptions in the UV[15] and is expected to bond exclusively through the π system, thus serving as a useful comparison to the behavior of pyrazine and pyridine.

The other systems, benzene[16] CO[17], O_2[18], and ethanol, were chosen for study when the preliminary investigations yielded very similar results. These gases were selected because the chemisorption behavior is fairly well characterized, and because they have no strong molecular transitions in the energy region of interest.

The results we report here indicate that, among the many possible modifications to the optical response of molecules chemisorbed on metal surfaces, a single mechanism is responsible for the spectral features in all the systems studied. The spectra of pyrazine, pyridine, naphthalene, and benzene are in fact nearly identical to those of CO, O_2, and ethanol, where the chemisorption chemistry should be quite different. Therefore, we propose that the optical absorption we observe for molecules chemisorbed on nickel (111) is evidence of a fundamental modification in the optical response of the metal itself.

II. EXPERIMENTAL

Apparatus

The stainless steel vacuum chamber used in these experiments is pumped by a titanium sublimation pump and a 400ℓ/s Varian Vacion pump in the triode configuration. Typical operating pressures are $1-2 \times 10^{-10}$ torr as measured by an uncorrected ionization gauge. The predominant background gases are H_2, Ar, CO, and CH_4, in order of decreasing abundance as measured by a UTI 100C quadrupole residual gas analyzer. The chamber is configured in two levels. The upper level contains the liquid helium-cooled experimental stage, LEED/Auger optics, quartz entrance and exit windows, an argon ion sputtering gun, variable leak valve to a gas inlet line, and observation ports. The lower level houses the sample heating stage, a tungsten filament, residual gas analyzer, ion gauge, and additional observation ports. The sample is moved between levels with a magnetically coupled linear/rotary motion manipulator.

The nickel single crystal sample was spark cut from a 3/8" diameter rod of 99.999+% purity (Materials Research Corp.) After a preliminary orientation of the surface within 2° of the (111) face by Laue X-ray backscattering, the back was ground parallel to the face. The 1/8" thick sample was then electron beam welded to a specially machined 99.99 +% purity polycrystalline nickel backing. The sample assembly was then carefully reoriented and polished to within 1° of the (111) face. During the final polish in a slurry of .05µ Al_2O_3, the surface was swabbed at 30 minute intervals with a solution containing glacial acetic, nitric, sulfuric and phosphoric acids in relative proportion 5:3:1:1 heated to 80°C. This etching procedure removed surface layers damaged during the stages of coarse polishing.

Once in the vacuum chamber, the crystal was cleaned with several cycles

of argon ion sputtering followed by extensive annealing. Typical cleaning

involved 15 minutes of 2 Kv argon ion sputtering at an angle near 60° from

the surface normal, 15 minutes annealing near 600°C, then an additional

5 minutes sputtering followed by a final anneal for 20-25 minutes. The sample

was heated by lowering the crystal-backing assembly into the prongs of an insulated

stage which can be raised to 5Kv above ground potential. A tungsten filament

located opposite the stage was heated to produce a high flux of thermally

ejected electrons which then cross the gap and strike the crystal backing.

Temperature measurements were made using an optical pyrometer. Typical operating

conditions were a 4Kv potential and a current of 7mA to bring the sample to

$600-700^{\circ}$C. After such a cleaning procedure, LEED and Auger analysis showed

highly ordered, clean nickel (111) surfaces.

During the experiments the crystal assembly was held in the copper end

of a liquid helium cryostat. A secure mount was provided by mating a dovetail

machined into the crystal backing with a female dovetail in the copper tip. A

small leaf spring pressing on the crystal backing prevented wobbling and produced

good thermal contact in the dovetail. Once in the holder, the manipulator

was unscrewed from the sample. This arrangement allowed sample cooling to

below 10K, as evidenced by continuous condensation of H_2 at 10^{-8} torr. Two

iron-doped gold/chromel thermocouples mounted on the cold tip provided

temperature estimates, but absolute measurements were prevented by the heating

of secondary junctions at the vacuum feedthrough by the cryostat gas return

heater.

A 75W high pressure X_e arc lamp in conjunction with a spex Doublemate

monochromator equipped with ruled gratings blazed at 2500Å produced light of

sufficient intensity to 2350Å free from broadband scattered light. The light
exiting the monochromator was collected with a quartz lens, reflected from
a MgF_2 coated aluminum mirror, and passed through a MgF_2 Rochon prism
input polarizer onto the sample surface. The reflected light passed through
the quartz analyzer polarizer and was detected by an EMI 9558Q photomultiplier.
The photomultiplier output was presented to a buffer amplifier of typical gain
100 before passing to the analog-to-digital converter for processing.

Two features of this system are considered extremely important. Both
entrance and exit windows were specially constructed of UV-grade quartz components
annealed at high temperature to minimize stress-induced birefringence. The
quartz components were then attached to a pyrex graded seal on a standard vacuum
flange, and, when mounted and under vacuum, display virtually no birefringence
throughout the range of experimental wavelengths. The second feature, believed
to be unique, is an optical path passing through holes in the LEED/Auger optics.
This was accomplished by electron discharge machining to prevent warpage of the
retarding grids. This arrangement allows optical studies of overlayers of
known periodicity and composition, thus eliminating errors in surface adsorbate
structures examined due to variations in local pressures during adsorption
in separate LEED/Auger and optical spectroscopic experiments.

The spectroscopic rotating analyzer ellipsometer used in these experiments
was built after a design by Aspnes. Detailed information regarding the operation,
calibration, and data analysis involved in using this type of instrument may
be found in references 19 and 20. Briefly, the elliptically polarized light
that exits the chamber passes through a polarizer rotating at 31.25 Hz, producing
a sinusoidally time-varying flux detected by the photomultiplier. The signal
is sent through a buffer amplifier to an ADAC model 1030 analog-to-digital

converter interfaced to a Digital Equipment Corp. PDP11/03 laboratory micro-computer. The analysis of this signal by the computer is triggered by optical encoder circuitry on the analyzer motor. Mounted on the shaft of the rotating analyzer is a nickel-plated, polished disc with 72 parallel cuts machined at equal intervals around the circumference. At one point on the disc, an additional hole is drilled between two cut-outs. Two optical encoders are aligned with this disc to provide 72 trigger points for data collection and a single trigger acting as the origin for the data triggers.

To normalize the spectrum to the intensity of the excitation source, the photomultiplier output is monitored by Kepco APH-2000M programmable high voltage supply, and the photomultiplier voltage is adjusted so that the average DC signal level stays constant over the entire wavelength region of interest. Signal averaging is achieved by programming the computer to collect data for a specified number of revolutions of the analyzer. The monochromator is then turned to the next wavelength by a computer-controlled stepping motor, and a delay is built into the program to allow for mechanical vibrations to decay and the photomultiplier supply to adjust to the new signal level.

Data Acquisition and Reduction

Following the final annealing of the crystal, the sample assembly is moved from the heating stage to the crystal stage. The cryostat assembly is moved into the optical path and the optical components are aligned. Due to the daily movement of the sample, the angle of incidence and beam positions on the input and output windows can vary significantly. The latter is not a problem, but the former is a major difficulty which will be discussed further below. If the experiments are to be performed at low temperatures, the sample is

cooled and a final alignment of the optics is often necessary due to contractions in the cryostat. After the system has been calibrated, a spectral scan on the bare surface is performed. The gas of interest is then admitted to the chamber and progress of the adsorption is monitored ellipsometrically at a wavelength where the overlayer is presumably transparent. A second spectral scan is then collected and the two data sets can be analyzed. If further treatments of the sample are to be done, they are all performed without moving any of the system components.

While a detailed systematic discussion of ellipsometry[21,22] is beyond the scope of this report, a brief introduction should serve as an aid to understanding the experiments and their subsequent interpretation. Linearly polarized light may be decomposed into electric field components parallel (p) and perpendicular (s) to the plane of incidence. Upon reflection from a surface, the final polarization state is, in general, elliptic due to changes in the relative amplitude and phase of the two component fields. Ellipsometry relates these changes to the complex dielectric response functions of the reflecting system. Inherent in the interpretation of ellipsometric data are a number of assumptions which for many systems appear to be reasonable. One assumes that the reflecting system can be described as a homogeneous, isotropic, semi-infinite substrate exhibiting a sharp planar boundary, covered by one or more layers of uniform thickness, also homogeneous and isotropic. This system is then embedded in some form of ambient surrounding. The applicability of this model has been challenged, especially in interpreting the behavior of thin molecular layers and sub-monolayer films on atomically clean surfaces. Several attempts have been made at describing the scattering of radiation by

atomic and molecular systems in a more rigorous fashion, yet for the general analysis of laboratory data they offer little prospect for routine applicability. Some extensions to anisotropic substrates and overlayers have been made, but they remain difficult to apply, and the bulk of ellipsometric data continues to be interpreted within this simplified framework (see reference 22).

The quantities measured in ellipsometry may be expressed as:

$$\rho \equiv \frac{\tilde{r}_p}{\tilde{r}_s} \equiv \tan \psi e^{i\Delta}$$

where $\tilde{r}_p$ and $\tilde{r}_s$ are the complex amplitude reflection coefficients for the electric field at the interface. In the simplified model described above, $\tilde{r}_p$ and $\tilde{r}_s$ are the Fresnel coefficients and are related to the optical properties of the overlayer, substrate and ambient, as well as the angle of incidence. For this model,

$$\frac{\tilde{r}_p}{\tilde{r}_s} = \left[\frac{\tilde{n}_1^2 \cos\phi_o - n_o (\tilde{n}_1^2 - n_o^2 \sin^2\phi o)^{1/2}}{\tilde{n}_1^2 \cos\phi_o + n_o (\tilde{n}_1^2 - n_o^2 \sin^2\phi_o)^{1/2}}\right] \left[\frac{\tilde{n}_o \cos\phi_o + (\tilde{n}_1^2 - n_o^2 \sin^2\phi_o)^{1/2}}{\tilde{n}_o \cos\phi_o - (\tilde{n}_1^2 - n_o^2 \sin^2\phi_o)^{1/2}}\right]$$

where $\tilde{n}_o$ is the refractive index of the ambient, $\tilde{n}_1$ is the complex refractive index of the substrate, and ϕ_o is the angle of incidence with respect to the substrate normal. For any layered system, the Fresnel coefficients for a given layer j can be determined as

$$\tilde{r}_{jp} = \frac{\tilde{n}_j \cos\phi_{j-1} - \tilde{n}_{j-1} \cos\phi_j}{\tilde{n}_j \cos\phi_{j-1} + \tilde{n}_{j-1} \cos\phi_j}$$

$$\tilde{r}_{js} = \frac{\tilde{n}_{j-1} \cos\phi_{j-1} - \tilde{n}_j \cos\phi_j}{\tilde{n}_{j-1} \cos\phi_{j-1} + \tilde{n}_j \cos\phi_j}$$

where now all refractive indices and angles are, in general, complex. For the

systems to be dealt with here, the three phase (ambient-overlayer-substrate)

ellipsometric equation can be expressed as

$$\rho = \tan\Psi\, e^{i\Delta} = \left[\frac{r_{1p}+r_{2p}e^{-iZ}}{1+r_{1p}r_{2p}e^{-iZ}}\right] \cdot \left[\frac{1+r_{1s}r_{2s}e^{-iZ}}{r_{1s}+r_{2s}e^{-iZ}}\right]$$

$$Z = (4\pi d/\lambda o)\ (\tilde{n}_1^2 - n_o^2\sin^2\phi_o)^{1/2}$$

where d is the thickness of the overlayer and λo is the vacuum wavelength of

light. For all of the results presented here, the incident beam was about

60° from the surface normal and linearly polarized at 30° from the plane

of incidence.

Unlike classical null ellipsometers, rotating analyzer systems of this

type measure $\tan\Psi$ and $\cos\Delta$ rather than Ψ and Δ directly. For the metal

systems investigated, the expected values of Ψ and Δ are such that there is

no ambiguity in converting from ($\cos\Delta$, $\tan\Psi$) to (Δ, Ψ) for further analysis.

The simplest type of analysis consists of the difference between bare metal

parameters ($\bar{\Delta}, \bar{\Psi}$) and the corresponding values for the covered metal at each

point in the spectrum. The difference functions $\delta\Psi=\Psi-\bar{\Psi}$ and $\delta\Delta=\Delta-\bar{\Delta}$ (the bar

indicating bare metal values) are, in general, complicated functions of the

overlayer dielectric properties and thickness. However, experience has

shown that most of the spectral features can be gleaned from these simple

functions without resorting to sophisticated analyses. Figure 1a shows

the result of $\delta\Delta$ and $\delta\Psi$ for a 10Å layer of condensed annealed pyrazine.

For comparison, 1 b demonstrates the result of analyzing for n and k. These

spectra also demonstrate the sensitivity of the instrument for moderate

and strong absorption features in very thin layers. (Notice the resolved

vibronic structure in the low energy transition.) As a standard tool,

difference spectra are not usually used to interpret spectral data. They

are extremely useful, though, in regions where the overlayers are transparent, where $\delta\Psi \cong 0$ and $\delta\Delta \propto d/\lambda_0$, so that the change in Δ can be used as a crude measure of the thickness of the overlayer during an adsorption.

Two factors in these experiments make rigorous analyses of the spectra difficult. The first involves uncertainty in the angle of incidence. For a given dielectric constant and wavelength of light, variations in the angle of incidence by as little as 0.01° have pronounced influence on the values of Ψ and Δ. Due to the nature of our sample mount, variations in the angle of incidence as large as 1° arise on a daily basis. Measurements of this angle are subject to errors of approximately $\pm 0.1^\circ$. Thus, the values of optical constants resulting from the analysis must not be regarded as absolute but used for defining spectral features and as a means of comparison between systems.

The second uncertainty in the analysis is in the thickness of the overlayer. Complete characterization of the overlayer requires three parameters: the real and imaginary parts of the refractive index, and the thickness of the layer. Ellipsometric measurements provide only two pieces of information, so a third measurement must be made or inferred. The most common solution is to make an ellipsometric measurement where the overlayer is assumed transparent. The remaining variables, n and d, can be uniquely determined, and the calculated thickness can then be used to calculate both n and k at other wavelengths. A second method[23] involves making measurements of Ψ and Δ at several thicknesses during the course of a deposition. A series of solutions over a range of n and k values is calculated which make the thickness a purely real quantity. When the solutions for two different thicknesses are plotted in n-k space, the intersections of the curves correspond to the

n and k values shared by both measurements. If the assumption is made that these n and k values are constant for all thicknesses, then the thickness of the overlayer at the end of the adsorption run can be calculated and used in the determination of n and k at different wavelengths. This approach has proven to be useful for a number of condensed layer systems, but for very thin layers and chemisorbed systems, this method has been found to be unreliable. The solution to this problem which was finally adopted in our analysis is a cautious comparison of the thickness of the overlayer expected from exposure times and molecular dimensions with that obtained by minimizing the absorption index in a region of expected transparency.

The frequency dependent complex refractive index represents the desired information about the response of the adsorbed overlayer, and the method used to obtain these values is straightforward. Each experimental spectrum terminates in a region where the overlayer is expected to be transparent. The values of Ψ and Δ measured for the bare and covered surface are used in a linear approximation expansion of the exact ellipsometric equations, which are applicable to layers where $d \ll \lambda$[22]. An initial guess is made for d and the complex refractive index is calculated. Successive values for d are examined until k is minimized. This value of the complex refractive index and thickness are then used in an iteration scheme based on a Taylor expansion of ρ in the complex refractive index. Iterations are performed until the deviation of the calculated ρ values from measured ρ values is within expected experimental error. This represents the first value of the overlayer refractive index. The next point in the spectrum is analyzed in the same way, using the best fit refractive index from the previous point as the starting value for the iteration. The complex index is calculated

at each point in the spectrum, and the final results are plotted as n and k vs. λ . Experience has shown that while the absolute values of n and k have a strong dependence on the chosen film thickness, the features in the spectrum remain undistorted until obviously erroneous thicknesses are used.

III. RESULTS

The studies of chemisorbed molecules were all performed at room temperature except where otherwise noted. Gases were deposited at pressures in the 10^{-8} torr range for several minutes until saturation occurred as measured by the change in the ellipsometric parameter Δ. Auger and LEED results were obtained after the ellipsometric spectra were recorded to minimize the effects of electron beam damage to the overlayers.

Condensed layers of gases were prepared by adsorption while the crystal was cooled to 15K. Thicknesses were monitored ellipsometrically, and in some cases the overlayers were annealed at 150K and cooled back to 15K before spectra were taken.

All the ellipsometric spectra were recorded with 0.5mm slits on the monochromator (10Å passband) and the data points were taken at 5Å intervals. Each point was averaged over 200 revolutions of the analyzer.

Pyrazine, Pyridine, Benzene, and Naphthalene on Ni(111)

The analyzed ellipsometric spectra of annealed condensed layers of pyrazine, pyridine, and naphthalene on Ni(111) at 15K are shown in Figures 2-4. Intense absorption peaks with vibronic structure are evident. The spectrum of a thick layer of condensed benzene showed no absorption maxima in this wavelength region, only the apparent onset of a large peak at higher energies. These spectra establish the positions of the molecular absorptions in the adsorbed layer and will be useful in interpreting the spectra of the corresponding chemisorbed species.

Pyrazine, pyridine, benzene, and naphthalene all appear to chemisorb on Ni(111) at room temperature. Saturation of the surface occurs after 3-5L exposures, with a final $\delta\Delta$ of about 0.5° - 0.7° at 3500Å. The adsorption of

pyridine leads to a very diffuse LEED pattern visible only at low electron
energies (figure 5). LEED spots for the chemisorbed pyrazine were very
indistinct and subject to very rapid deterioration in the electron beam.
Naphthalene on the other hand produces very clear, reproducible patterns
which would deteriorate after longer beam exposures. From an initial set
of rings surrounding each clean surface spot, annealing to 350K produces
the pattern seen in figure 6. Although we make no assignment of these
patterns, similar results were obtained on the Pt(111) surface.[24]

The spectrum of each of these chemisorbed molecules is shown in Figures 7-10.
Each absorption spectrum is dominated by one large, broad feature, which
is centered at 2850Å in the case of pyrazine and benzene, and at 3050Å
for chemisorbed pyridine and naphthalene. None of the molecules studied
exhibited any absorption features in the visible region of the spectrum.

CO, O_2, Ethanol on Ni(111)

The chemisorption of CO on Ni(111) yielded the familar LEED pattern[17]
after saturation at 3L. The final $\delta\Delta$ was 0.6° monitored at 3000Å. The UV
absorption spectrum is shown in Figure 11 and consists of a large, broad
peak centered at 2800Å.

Adsorption of O_2 at room temperature appears to undergo a rapid chemi-
sorption phase ($\delta\Delta \sim 0.2^\circ$ at 5000Å, p(2x2) LEED pattern develops after 1.5L).
After this initial stage, a slow oxygen uptake is indicated by the ellipsometer,
with a final $\delta\Delta \sim 2.0^\circ$ and a LEED pattern characteristic of NiO after 300L.
The analyzed spectrum of chemisorbed O_2 is shown in figure 12, and again a
broad feature at 2900Å is prominent. Prolonged exposure to form the NiO

had two effects on the analyzed spectrum. The magnitude of the analyzed peak was markedly increased and the actual peak position was shifted to higher energy as seen in figure 13.

At room temperature, exposure of the crystal to ethanol leads to a disordered chemisorbed phase, with $\delta\Delta \cong 0.3^\circ$ at 5000Å. The absorption spectrum of this species is shown in figure 14 and exhibits a peak at 2750Å. For comparison, a spectrum of a 100Å thick layer of ethanol condensed on Ni(111) at 80K is shown on the same scale. No evidence of an absorption peak is visible in the condensed layer spectrum.

IV. DISCUSSION

The electronic spectra of thick, annealed layers of pyrazine, pyridine, and naphthalene condensed on nickel(111) show intense absorption peaks with sharp vibronic structure. As reported earlier for condensed pyrazine[9], the peak energies and vibrational spacings agree well with those reported for the respective bulk crystals. So, for the case of weak interaction with the metal, it appears that the adsorbed molecules retain their electronic structure and are only slightly perturbed by the metal surface.

Contrasting with this behavior are the results of these molecules chemisorbed on nickel(111). The ultraviolet absorption spectra of all the molecules studied are dominated by a single large broad transition centered between 2800Å and 3100Å. The similarity in peak position and shape for all these spectra suggests that, in the chemisorption process on nickel, one feature of the bond formation is common to all the systems and is responsible for the appearance of the new optical absorption. Thus it is likely that, due to the wide range of adsorbate properties and surface chemistry, the absorption peak is evidence of an intrinsic change in the optical response of the metal. However, the possibility that different mechanisms for each molecule may be involved cannot be ruled out, so an assessment of each of the various possible origins of this peak must be made.

For the aromatic molecules which were studied, the most attractive explanation for chemisorption-induced absorption in the 4eV range is a molecular $\pi\pi^*$ type transition such as that observed in the spectra of

condensed adlayers. Evidence of singlet valence molecular transitions

in chemisorbed systems has been observed in ELS studies of pyridine on

Ir(111)[12] and CO on Ni(100)[25] and on Ni(111)[5]. In order for such an

excitation to lie in this energy range, the π^* orbital must be unoccupied,

i.e., lie above the Fermi level of the metal, and the energy difference

between the π and π^* orbitals must not be increased upon chemisorption

to the metal. UPS measurements of pyridine and benzene on Cu(110)[26] and

of benzene on Ni(111)[11] locate the filled π states of the absorbate about

4eV below the Fermi level, so an excitation to an empty π^* orbital just

above the Fermi energy would lead to an absorption near 2800Å. An estimate

of the possibility of a filled π orbital within 4eV of the Fermi level

for other molecules on nickel can be made by following the analysis of

Demuth and Eastman[11]. The results of their photoelectron studies indicate

that, with the exception of those molecular orbitals directly involved

in bonding, the adsorbate levels are shifted uniformly upon adsorption

and correlate well with gas phase photoelectron data. Using the gas phase

photoelectron spectrum and an estimate of this "relaxation shift" and

the work function change upon chemisorption, the placement of the Fermi

level with respect to the filled adsorbate levels can be approximated.

Assuming that the molecules bond so that the π system is relatively unperturbed,

an analysis using the photoelectron spectra of pyrazine and pyridine,[27]

a relaxation shift of 3eV, and $\Delta\phi \simeq 2eV$, places the highest filled π orbital

about 4eV below the Fermi energy, making possible a $\pi\pi^*$ transition at 4.5eV

(see figure 15).

Several objections arise, however, in attempting to assign the observed

optical absorption to a molecular $\pi\pi^*$ transition. First of all, only those

molecules which have excited states in the free molecule lying in this energy

range would be likely to exhibit this transition in the chemisorbed species.
Of the adsorbates studied, only pyrazine, pyridine, and naphthalene have
these states. Secondly, bonding of these molecules through their π systems
would shift the π orbital to higher binding energy, and thus the absorption
would be blue-shifted, perhaps even out of our accessible wavelength region.
Evidence from XPS measurements tends to indicate d-π bonding for
pyridine and benzene on nickel films[28], although metal bonding through
the nitrogen lone pairs of pyrazine and pyridine occurs in nickel complexes[29]
and may in fact occur on nickel(111)surfaces.

Another, more plausible, explanation for the observation of a broad,
featureless absorption peak is a charge transfer band. Charge transfer
transitions in this energy region are common in metal complexes, and absorptions
have been assigned to metal $\rightarrow$ ligand charge transfer for CO on Ni(111)
(6eV)[5], benzene and pyridine on Ir(111) (4-5eV)[12], and ethylene on Cu films
(5.4 eV)[8]. Once again, though, this effect is likely only for those adsorbates
which have low-lying empty orbitals, such as CO and the aromatic molecules.
One would expect, too, that charge transfer bands would have significantly
different characteristics for adsorbates of such different electron affinity
and geometry. The energy and intensity of charge transfer transitions
depend very strongly on the energy difference between and overlap of the
donor and acceptor orbitals[30], and it is unlikely that these should be identical
for orbitals of CO and those of benzene or naphthalene.

Another alternative explanation of the spectrum is that the extent
of electron transfer in the metal-ligand species is so great that the spectrum
is in fact that of an ionic complex and thus might bear little resemblance

to that of the parent molecule. Such behavior has been postulated to explain the adsorption-induced absorptions in the spectra of H_2 chemisorbed on Cu[8] and rare gases on Au, Al, and Mg[6,7]. If considered separately, such a rationalization would be attractive for explaining the behavior of chemisorbed oxygen as it passes from the chemisorbed system, through nucleation, and finally to a thin layer of NiO. This is certainly supported by the spectrum obtained for the final NiO layer which is in excellent agreement with the spectrum of single crystal NiO[31] (see figure 13).

In the final analysis, the striking similarity of the spectra of all the adsorbate systems studied make the argument for a chemisorption-induced change in the metal spectrum a compelling one. The broad range of adsorbate properties, from electron donors to electron acceptors, from small molecules to large aromatic molecules, points to a change in the metal as the factor common to all. It is not possible to attribute the modification of the metal response to any one particular mechanism, since theoretical and experimental work in this area is so limited. Once again, a careful judgement of the extent of the possible effects is in order.

The feature observed in the spectra of the chemisorbed overlayers is almost certainly not caused by a change in a collective mode of the metal due to the change of the dielectric constant at the boundary. The bulk and surface plasmon excitations of nickel lie at much higher energies[32], and no effect is observed for physisorbed or condensed layers which should also change the dielectric function at the surface. Such pronounced effects have been observed by us in the spectra of adsorbed overlayers on silver single crystal surfaces, where the bulk and surface plasmons lie in the near ultraviolet[33].

An intriguing explanation for the appearance of the absorption peak
is an adsorption-induced change or creation of a surface state or resonance.
In fact, photoemission experiments by Himpsel and Eastman[34] indicate an s-p-like
intrinsic surface state on nickel(111). Adsorption of gases seems to shift
this state to higher binding energy, and eventually the emission from this
state disappears for even submonolayer coverages. A surface state on the
Cu(111) surface has been observed to shift to lower energy upon adsorption
of an electron donor (Cs) and to higher energy when an electron acceptor (O_2)
is adsorbed[35]. Similar surface states are observed for Ag(111)[36] and Au(111)[37].

Despite the evidence of an intrinsic surface state on Ni(111) which is
highly sensitive to the presence of adsorbates, it is difficult to rationalize
the appearance of an absorption peak upon chemisorption with the removal
of the surface state. In their analysis of surface reflectance measurements
of H_2 on tungsten, Restorff and Drew[4] postulated the removal of a metal
state to account for apparent negative resonances in the reflectivity.
O'Handley and Burge[38] attributed a peak in their ellipsometric spectrum
of O_2 on Ag films at 2.4eV to a transition from a filled metal state to a
chemisorption-induced surface state. However, there is no additional justifi-
cation for their assignment, and any assertion of similar behavior on Ni(111),
especially identical behavior for all the adsorbates studied, would also
be tenuous.

The exact effect of a chemisorbed overlayer on the optical response of
the metal surface is difficult to specify. As described in the introduction, the
presence of an adsorbate would change the potential felt by the metal electrons
at the surface, changing the response of those electrons to electric fields
normal to the surface. The contribution of non-local dielectric response to

the total dielectric function is an open question even for the clean

surface[39], so changes in that contribution upon chemisorption would have

an undetermined effect.

The most plausible explanation for the chemisorption-induced absorption

peak involves recognizing that this new absorption occurs in the same

energy region as intrinsic interband transitions in the bulk metal[40].

Band structure calculations and computation of the optical conductivity

for nickel suggest that the strong absorption feature beginning near 4eV

has contributions throughout the Brillouin zone.[41,42] Thus, while this absorption

can not be linked to processes near a single symmetry point or line,

calculations indicate the importance of optical processes involving the

lowest energy d band and final states just above the Fermi energy. The

normal condition of translational invariance in crystalline solids leads to

the requirement that direct optical processes involve only states of identical

crystal momentum; thus, only vertical excitations are allowed. Indirect, or

non-vertical, processes are allowed only through the participation of phonons

in order to conserve momentum. While indirect transitions are extremely

important in semiconductors near the absorption threshold, the optical

response of metals is dominated by the many strongly allowed direct excitations.

However, near the surface of the solid, the translational invariance

normal to the surface is clearly disrupted. In this region, therefore,

optical processes may occur where crystal momentum components normal to

the surface are not strictly conserved, while conservation of momentum

components parallel to the surface is still required.

Chemisorption is likely to disrupt the symmetry of the surface potential

in directions parallel to the surface. This loss of symmetry would completely

relax the requirement of electron crystal momentum conservation for allowed optical processes. Thus, optical transitions to points in the zone near direct transitions would become possible, leading to new absorptions near the energy of momentum-conserving excitations (see figure 16). The extent and nature of this symmetry disruption probably varies from one adsorbate to another, but the energy and intensity of the newly allowed transitions would be more sensitive to the joint density of states for the participating bands. Thus, the general appearance and energy of the chemisorption-induced absorption peaks could be nearly the same for all adsorbates.

While the results of this investigation cannot conclusively determine the origin of the observed spectral feature, they do indicate that a change in the optical response of the metal occurs upon chemisorption. Theoretical support for this model is unavailable due to present limitations in calculating the optical properties of solids. The only similar experimental evidence is provided by the electron energy loss studies of CO on Ni(111) by Rubloff and Freeouf[5]. A loss feature near 4eV is indicated, yet was not interpreted in their analysis. We suggest that this energy loss arises from the same change in the metal spectrum which leads to the absorption peak observed in our optical studies. Further experimental endeavors are required before final assignment of this peak can be made.

V. CONCLUSION

Spectroscopic investigation of the chemisorbed species pyrazine, pyridine, naphthalene, benzene, oxygen, carbon monoxide and ethanol on the Ni(111) surface reveal a single absorption feature in the 2800-3000Å wavelength region common to all systems. The origin of this enhanced absorption is believed to be a modification of the optical response of the substrate induced by the chemisorption process. An exact determination of the processes involved in the metal is not possible, but the proximity of the feature to known interband absorption processes in nickel suggests a perturbation of the symmetry of the surface layers leading to a relaxing of momentum conservation requirements for transitions originating in the surface region.

VI. ACKNOWLEDGEMENT

References

1. G. W. Rubloff, J. Anderson, M. A. Passler, and P. J. Stiles, Phys. Rev. Lett. 32, 667 (1974)

2. J. Anderson, G. W. Rubloff, M. A. Passler, and P. J. Stiles, Phys. Rev. B10, 2401 (1974)

3. M. A. Passler and P. J. Stiles, J. Vac. Sci. Technol. 15, 611 (1978)

4. J. B. Restorff and H. D. Drew, Surf. Sci. 88, 399 (1979)

5. G. W. Rubloff and J. L. Freeouf, Phys. Rev. B17, 4680 (1978)

6. J. E. Cunningham, D. Greenlaw, J. L. Erskine, R. P. Layton, and C. P. Flynn, J. Phys. F7, L281 (1977)

7. J. E. Cunningham, D. Greenlaw, C. P. Flynn, and J. L. Erskine, Phys. Rev. Lett. 42, 328 (1979)

8. M. Moskovits and P. McBreen, J. Chem. Phys. 68, 4992 (1978)

9. C. B. Harris, D. A. Zwemer, A. R. Gallo, and H. J. Robota, Surf. Sci., 85, L205 (1979)

10. J. D. E. McIntyre, "Optical Reflection Spectroscopy of Chemisorbed Monolayers", in Optical Properties of Solids: New Developments, B. O. Seraphin, ed., North-Holland, 1976.

11. J. E. Demuth and D. E. Eastman, Phys. Rev. B13, 1523 (1976)

12. F. P. Netzer, E. Bertel, J. A. D. Matthew, Surf. Sci., 92, 43 (1980)

13. I. Suzuka, N. Mikami, M. Ito, J. Mol. Spec., 52, 21 (1974)

14. K. K. Innes, J. P. Byrne, and I. G. Ross, J. Mol. Spec. 22, 125 (1967)

15. D. S. McClure and O. Schnepp, J. Chem. Phys., 27, 1575 (1955)

16. S. Lehwald, H. Ibach, and J. E. Demuth, Surf. Sci., 78, 577 (1978) and references therein

17. H. Conrad, G. Ertl, J. Küppers, and E. E. Latta, Surf. Sci., 57, 475 (1976) and references therein

18. P. R. Norton, R. L. Tapping and J. W. Goodale, Surf. Sci., 65, 13 (1977) and references therein

19. D. E. Aspnes and A. A. Studna, App. Opt. 14, 220 (1975)

20. D. E. Aspnes, J. Opt. Soc. Am. 64, 812 (1974)

21. D. E. Aspnes, "Spectroscopic Ellipsometry of Solids", in _Optical Properties of Solids: New Developments_, B. O. Seraphin, ed. North-Holland, 1976

22. R. M. A. Azzam and N. M. Bashara, _Ellipsometry and Polarized Light_, North-Holland, 1977

23. M. Malin and K. Vedam, Surf. Sci., _56_, 49 (1976)

24. J. L. Gland and G. A. Somorjai, Surf. Sci., _38_, 157 (1973)

25. K. Akimoto, Y. Sakisaka, M. Nishijima and M. Onchi, Surf. Sci., _88_, 109 (1979)

26. B. J. Bandy, D. R. Lloyd and N. V. Richardson, Surf. Sci., _89_, 344 (1979)

27. R. Gleiter, E. Heilbronner, and V. Hornung, Helv. Chim. Acta, _55_, 255 (1972)

28. K. Kishi, F. Kikui, and S. Ikeda, Surf. Sci., _99_, 405 (1980)

29. M. Goldstein, F. B. Taylor, and W. D. Unsworth, J. Chem. Soc., Dalton Trans., 418 (1972)

30. J. N. Murrel, Quart. Rev., _15_, 191 (1961)

31. R. J. Powell and W. E. Spicer, Phys. Rev. B6, 2182 (1970)

32. B. Heimann and J. Holzl, Z. Naturforsch. 27A, 408 (1972)

33. Unpublished results.

34. F. J. Himpsel and D. E. Eastman, Phys. Rev. Lett., _41_, 507 (1978)

35. S. A. Lindgren and L. Wallden, Surf. Sci., _89_, 319 (1979)

36. P. Heimann, H. Neddermeyer and H. E. Roloff, J. Phys. C10, L17 (1977)

37. G. V. Hansson and S. A. Flodström, Phys. Rev. B17, 473 (1978)

38. R. C. O' Handley and D. K. Burge, Surf. Sci., _48_, 214 (1975)

39. K. L. Kliewer, Surf. Sci., _101_, 57 (1980)

40. P. B. Johnson and R. W. Christy, Phys. Rev. B9, 5056 (1974)

41. D. G. Laurent, J. Callaway and C. S. Wang, Phys. Rev. B20, 1134 (1979)

42. C. S. Wang and J. Callaway, Phys. Rev. B9, 4897 (1974)

Figure Captions

Figure 1 a: The result of a simple difference spectrum ($\delta\Delta, \delta\Psi$) for a 10Å thick, condensed and annealed layer of pyrazine on Ni(111). $\delta\Psi$ reflects the absorbing properties of the layer while $\delta\Delta$ is most sensitive to the refractive index.

Figure 1 b: Absorbance calculated from an iterative analysis assuming a 10Å thick layer. Compare the vibronic structure with that of a thick layer in figure 2.

Figure 2:   The analyzed absorption spectrum for a 40Å thick condensed, annealed pyrazine layer on Ni(111).

Figure 3:   The analyzed absorption spectrum for a 25Å thick condensed, annealed layer of pyridine on Ni(111).

Figure 4:   The analyzed absorption spectrum for a 50Å thick condensed, annealed layer of naphthalene on Ni(111).

Figure 5:   The LEED pattern of pyridine chemisorbed on Ni(111) at room temperature. The beam energy is 66eV. (a) Photograph of the diffraction pattern. (b) Sketch of the pattern. Nickel diffraction spots are indicated by solid circles. Spots due to chemisorbed pyridine are indicated by the open outlines.

Figure 6:   The LEED pattern of naphthalene chemisorbed on Ni(111) at room temperature after annealing at 80°C. The beam energy is 52eV. (a) Photograph of the diffraction pattern. (b) Sketch of the pattern. Nickel diffraction spots are indicated by solid circles. Spots due to chemisorbed naphthalene are indicated by solid and open ovals.

Figure 7:   The analyzed absorption spectrum for chemisorbed pyrazine on Ni(111).

Figure 8:   The analyzed absorption spectrum for chemisorbed pyridine on Ni(111).

Figure 9:   The analyzed absorption spectrum for chemisorbed benzene on Ni(111).

Figure 10:   The analyzed absorption spectrum for chemisorbed naphthalene on Ni(111).

Figure 11:   The analyzed absorption spectrum for chemisorbed CO on Ni(111).

Figure 12:   The analyzed absorption spectrum for chemisorbed oxygen on Ni(111).

Figure 13:   The analyzed spectrum of epitaxial NiO formed after prolonged exposure of the Ni(111) surface to oxygen.

Figure 14:   The analyzed absorption spectra of chemisorbed ethanol (upper curve) and a 100Å layer of condensed ethanol (lower curve), shown on the same scale for comparison.

Figure 15:   Summary of vertical ionization potentials of gas-phase and chemisorbed pyridine, showing the filled π orbital for the chemisorbed species within 4.5eV of the Fermi energy of nickel. The gas-phase data are taken from Ref. 27. The data for the chemisorbed species and the orbital assignments are taken from the pyridine/Cu(110) study by Bandy, et.al. (Ref. 26). The work function change is that of pyridine on Pt(111) (Ref. 24). Using the analysis suggested by Demuth and Eastman (Ref. 11), the orbital energies of the chemisorbed molecule are shifted uniformly so that the ionization potentials of the core orbitals match those of the gas-phase pyridine. The "bonding shift" of the $7a_1$ (n) orbital is shown, and a transition from the $1a_2$ (π) orbital to a final state just above E_F (Ni) would occur at about 4.5eV.

Figure 16 a: The band structure of nickel calculated by Wang and Callaway[42].

Figure 16 b: The solid arrow indicates a vertical transition with a large momentum component parallel to the (111) direction. The dashed arrows indicate nonvertical transitions of nearly equal energy and (111) momentum component with the addition of momentum components parallel to the (111) face.
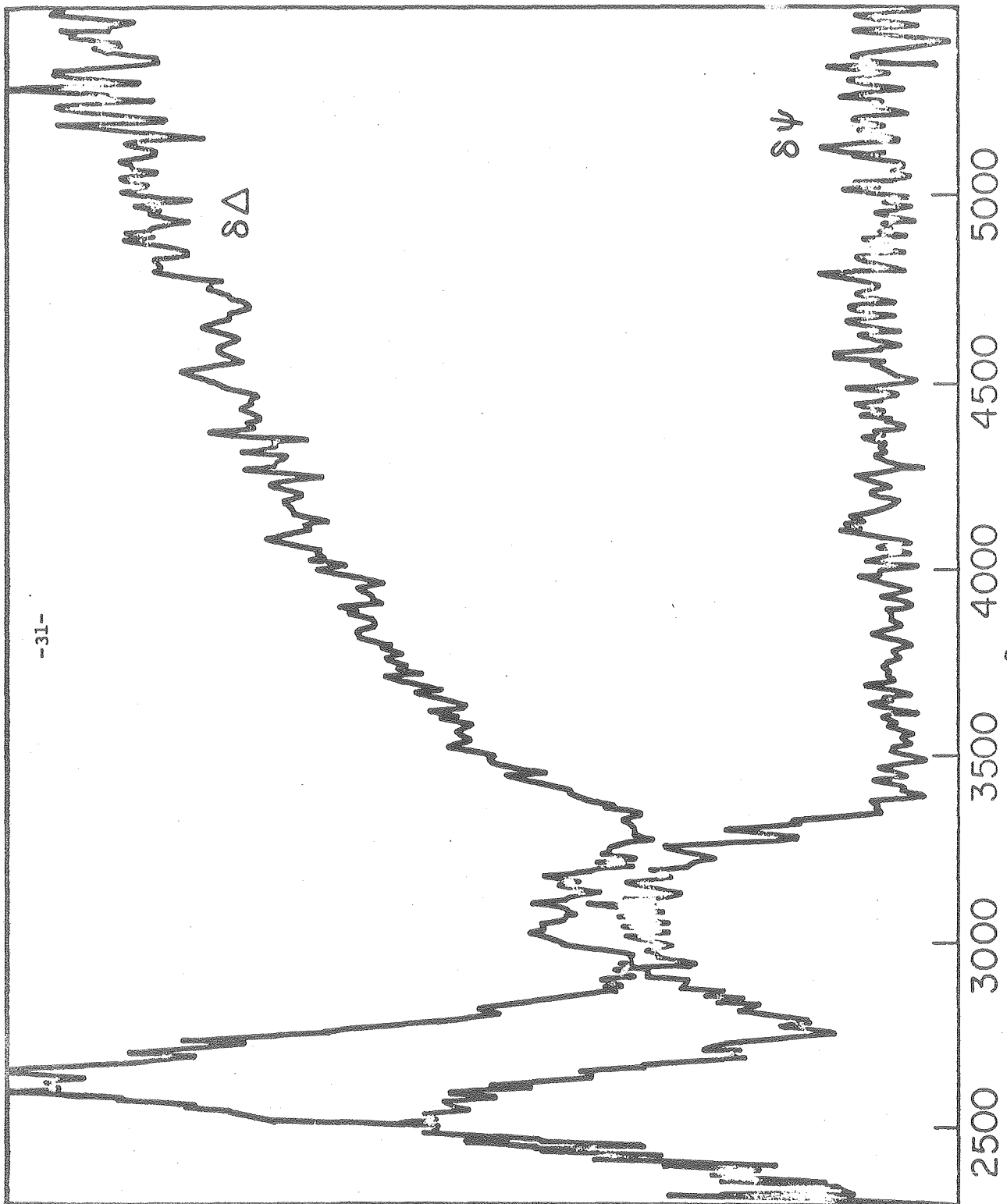
Figure 1.6

λ(Å)

$\delta\Delta$

$\delta\psi$

Absorbance

λ (Å)

2500 3000 3500 4000 4500 5000

FIGURE 1 b

-33-

Figure 2

ABSORBANCE

λ (Å)

XBL808-5820

Absorbance

λ (Å)

Figure 4

WBI00-5574
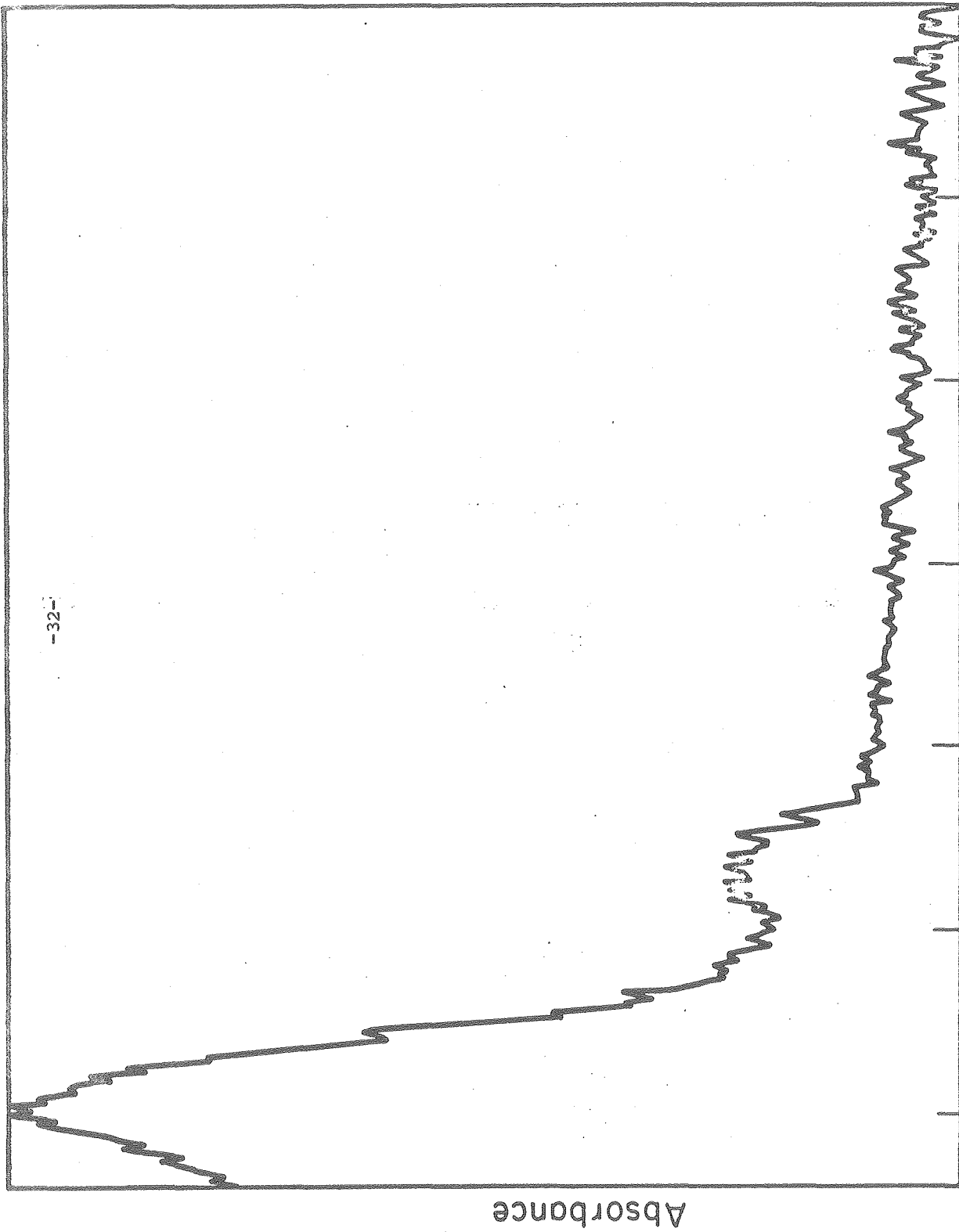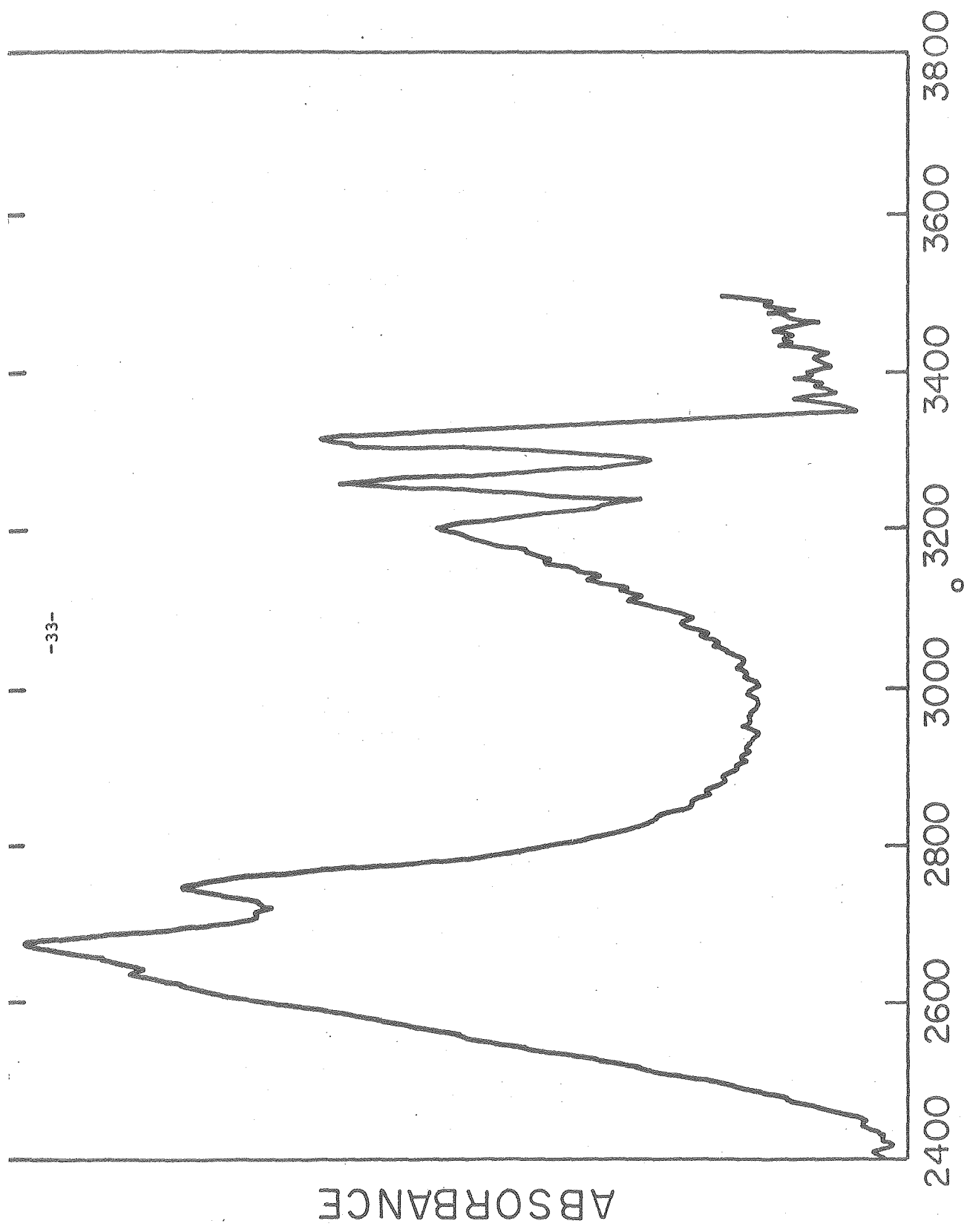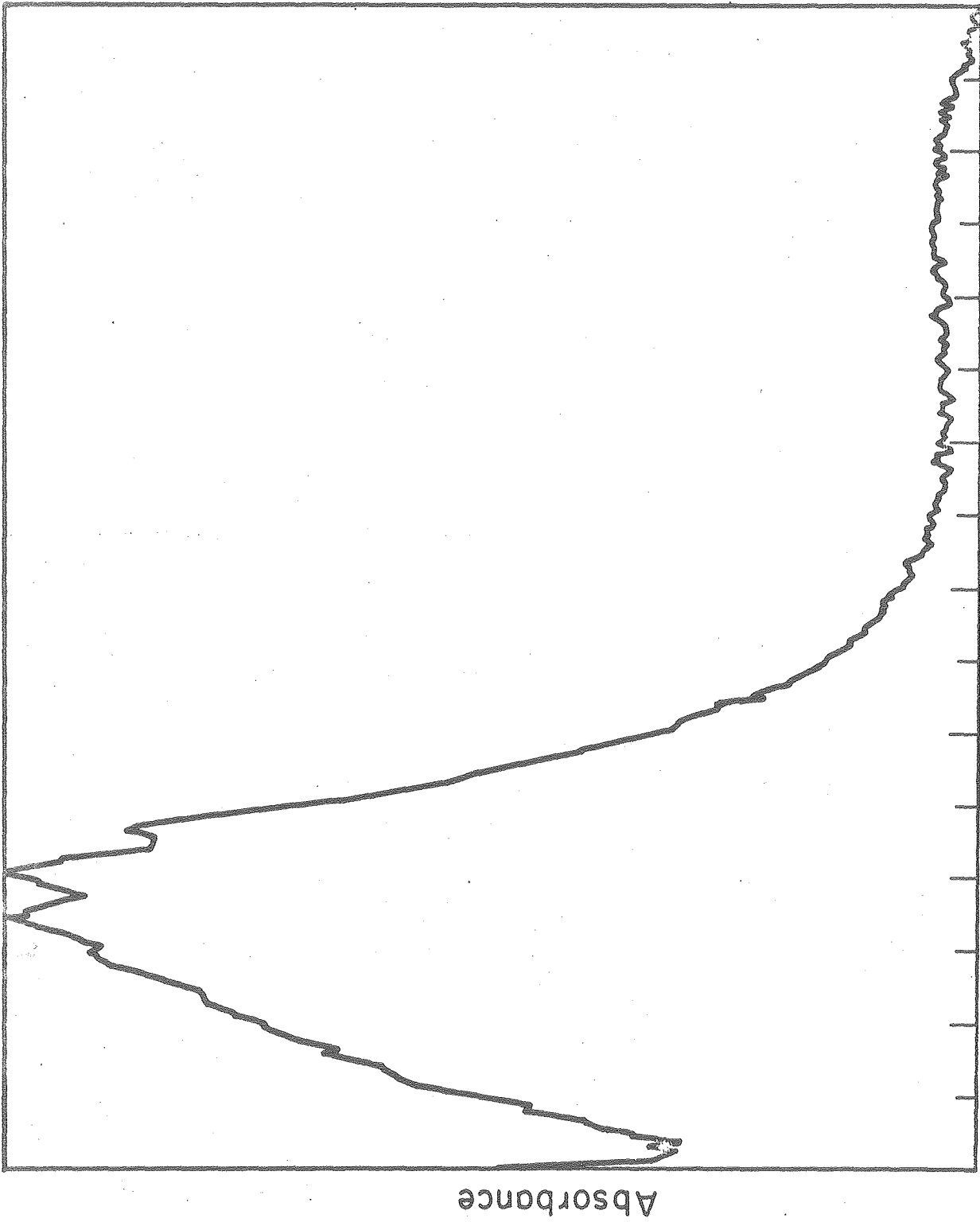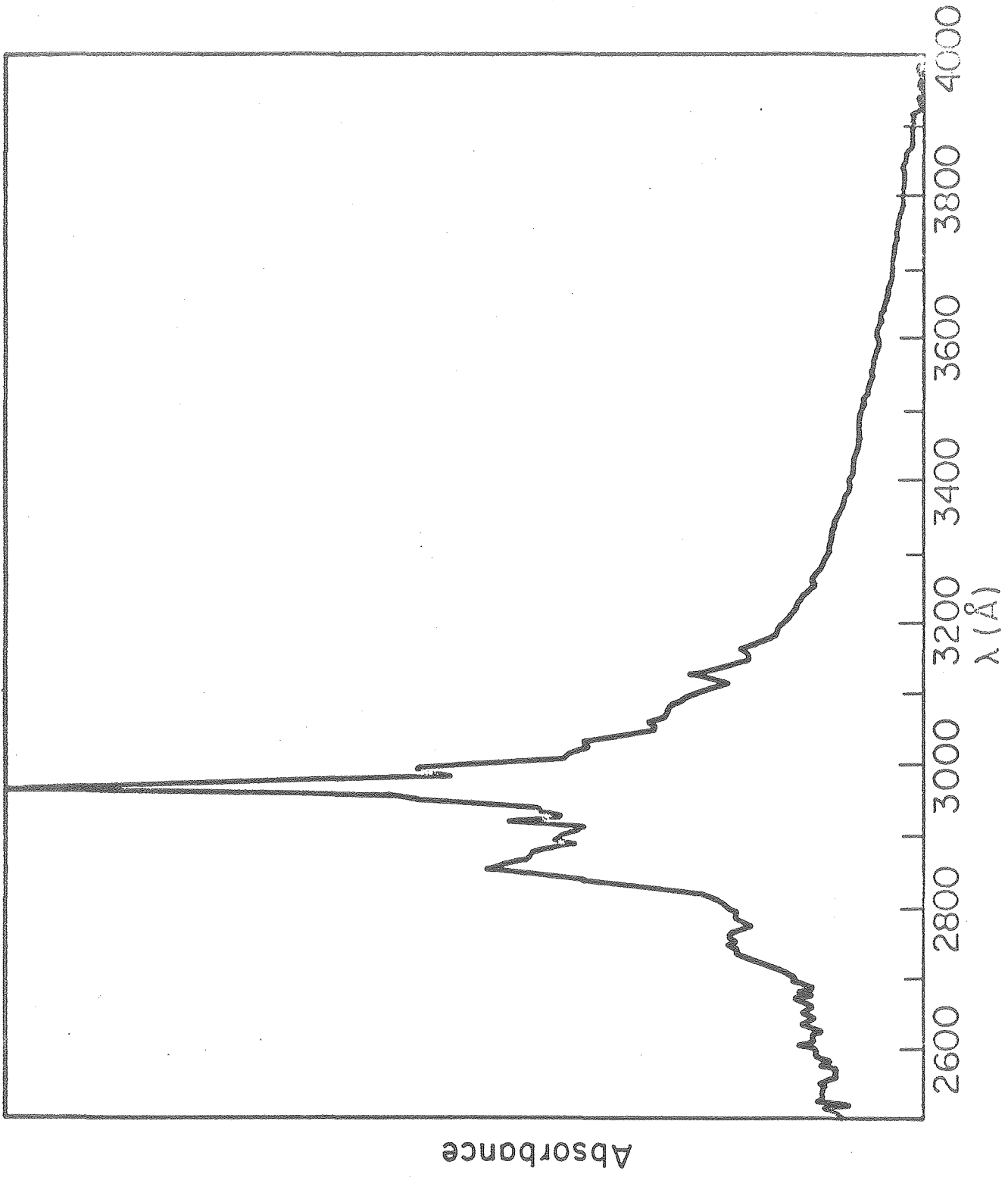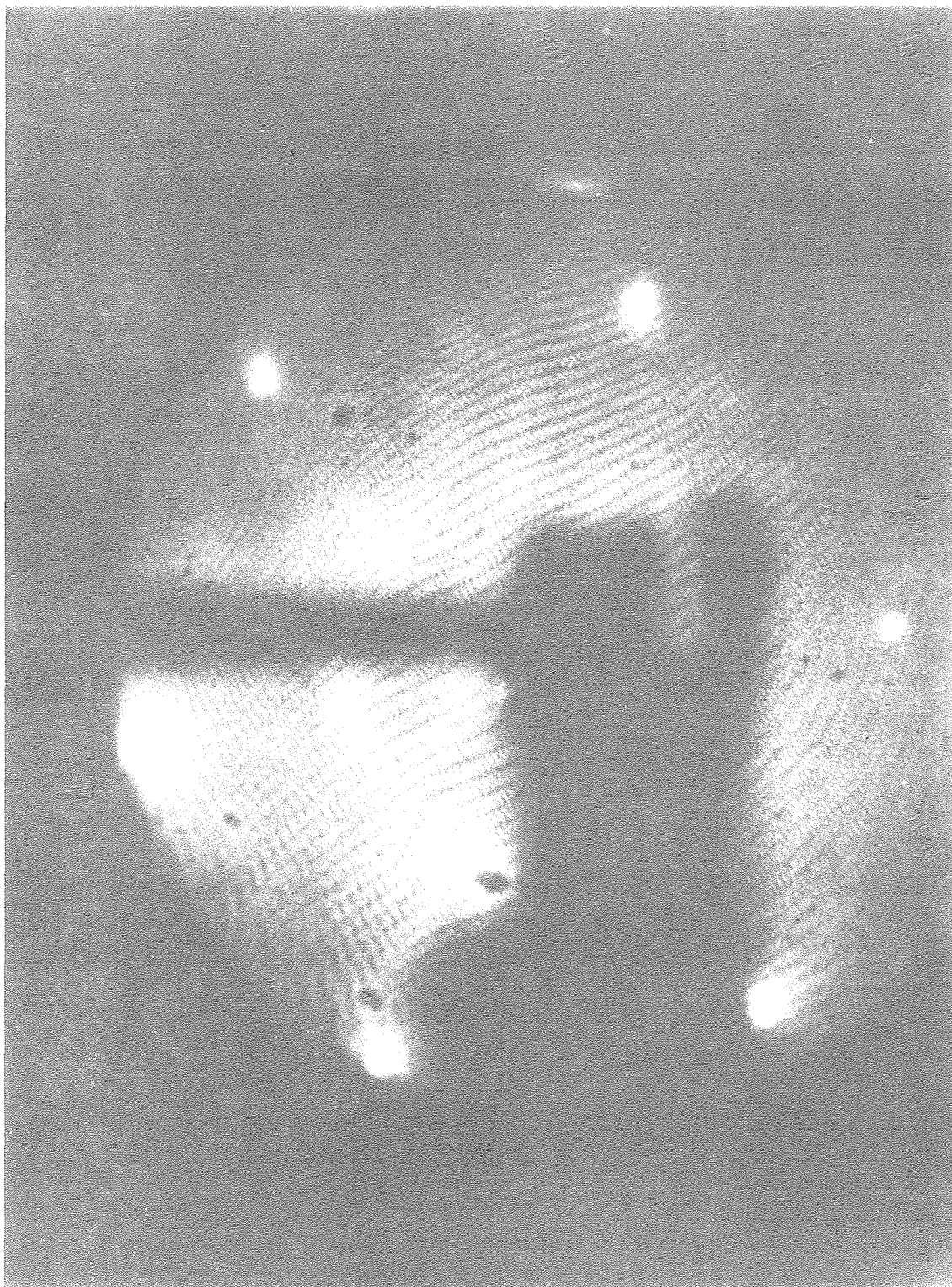
Figure 5a   XBB811-802
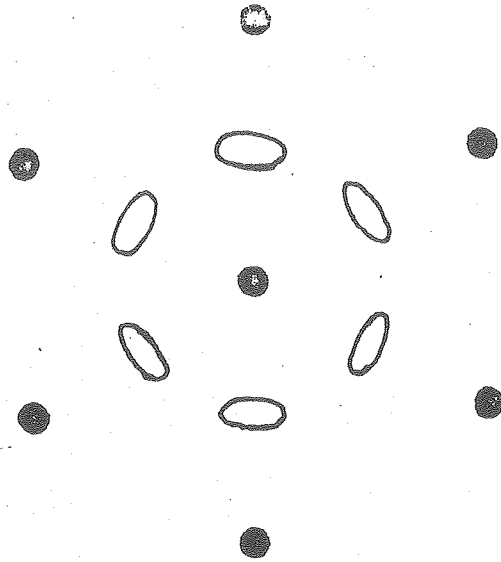
XBL 811-7806

Figure 5b
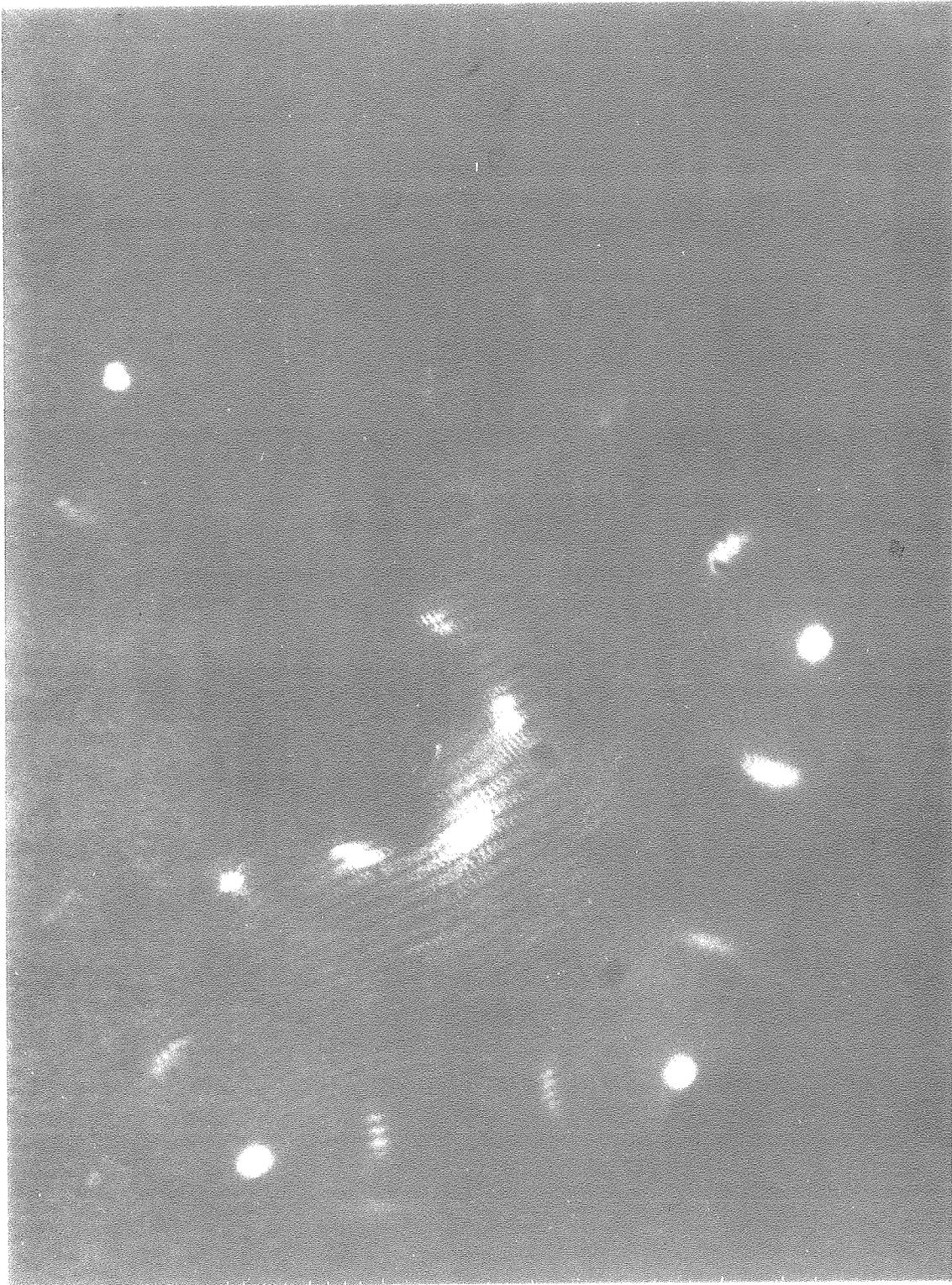
Figure 6a

XBL 811-7805
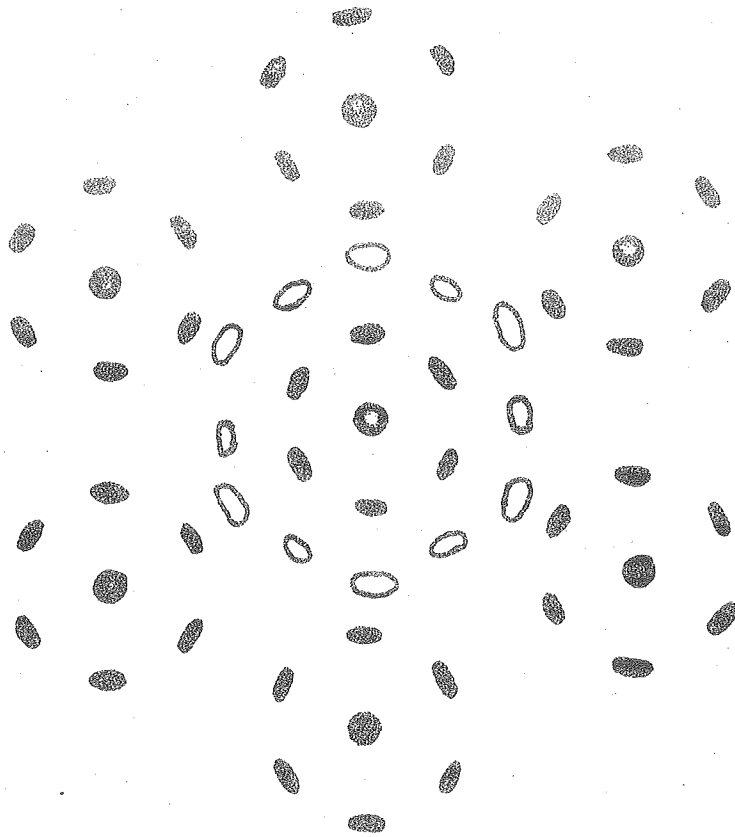
Figure 6b
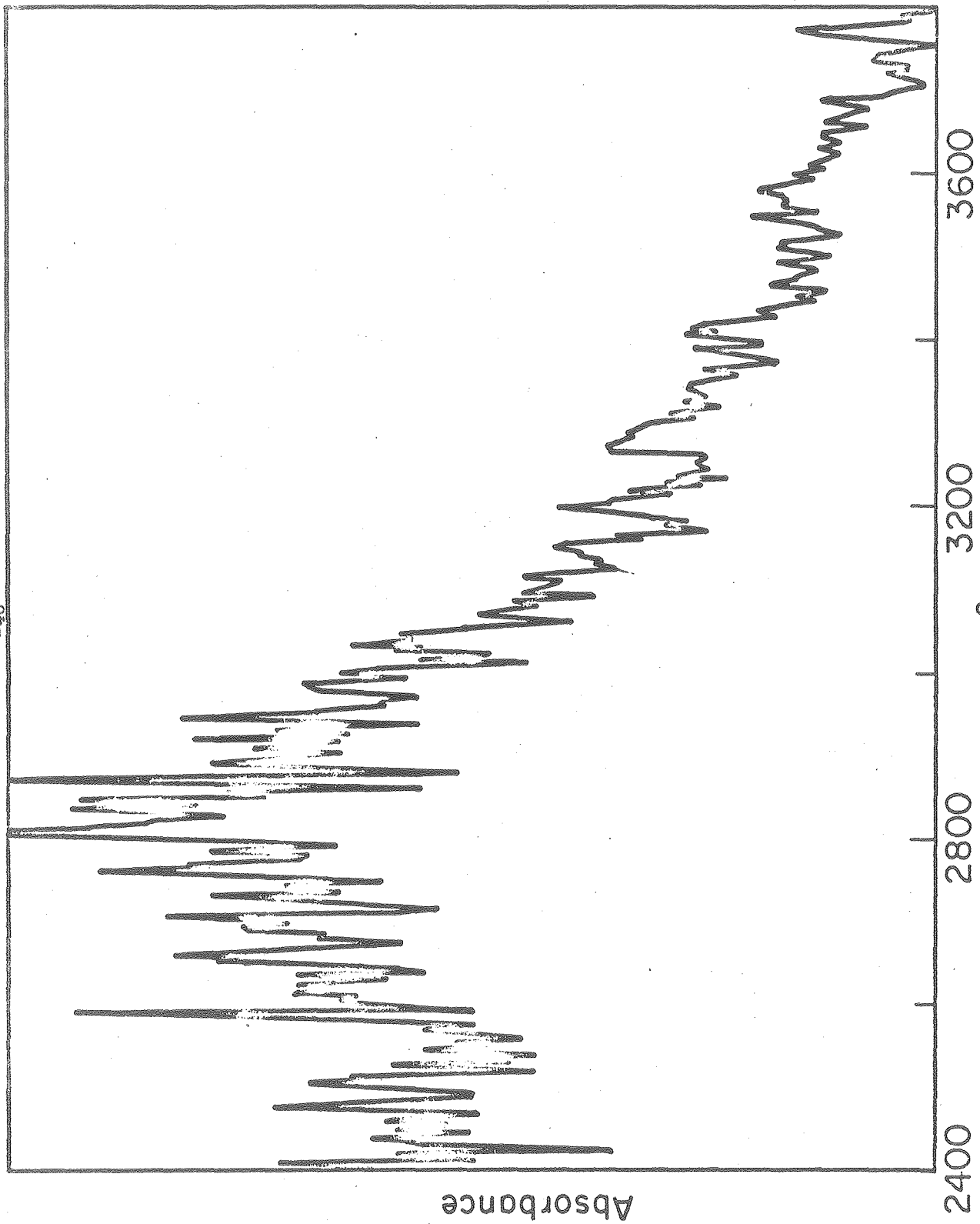
Absorbance
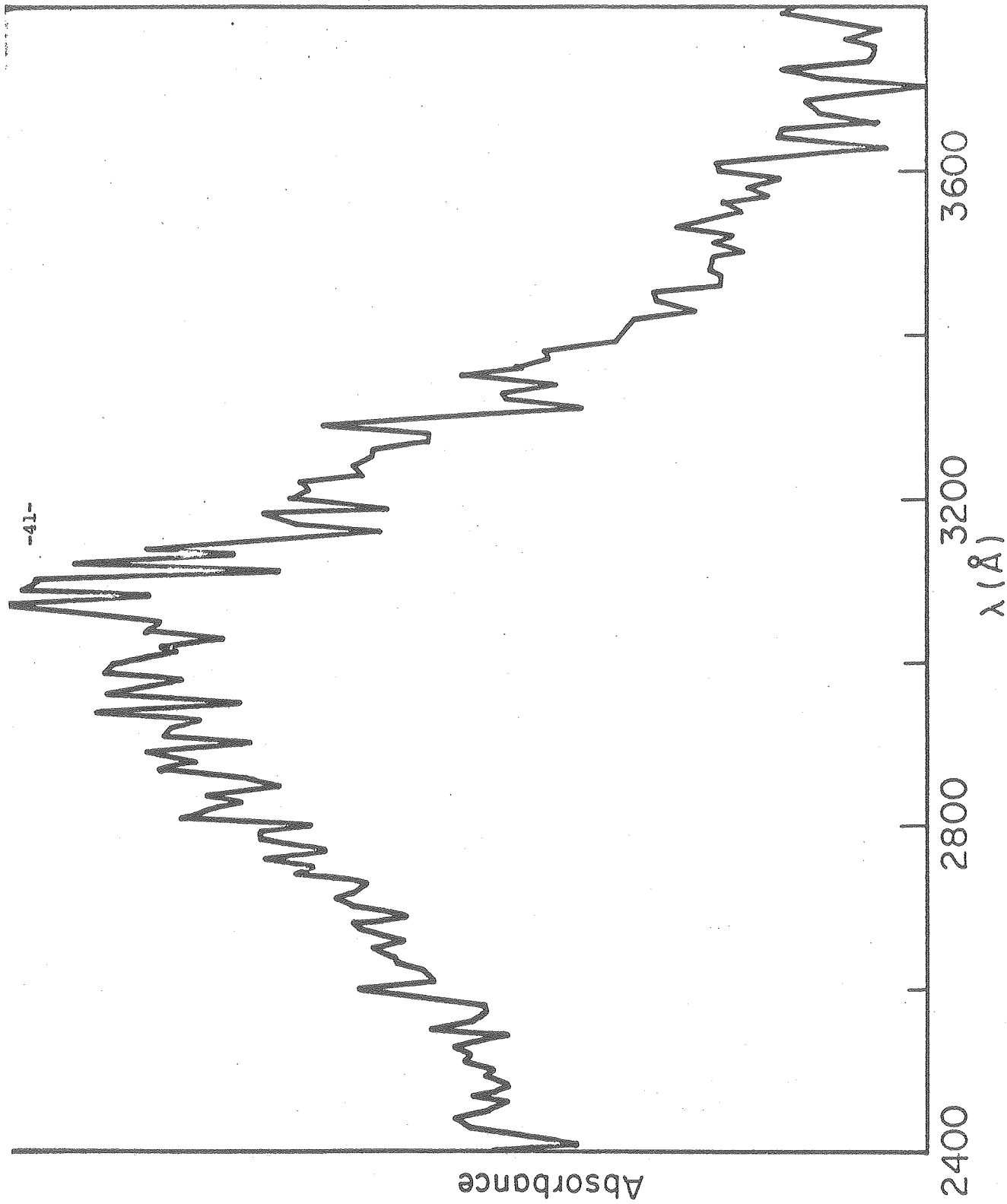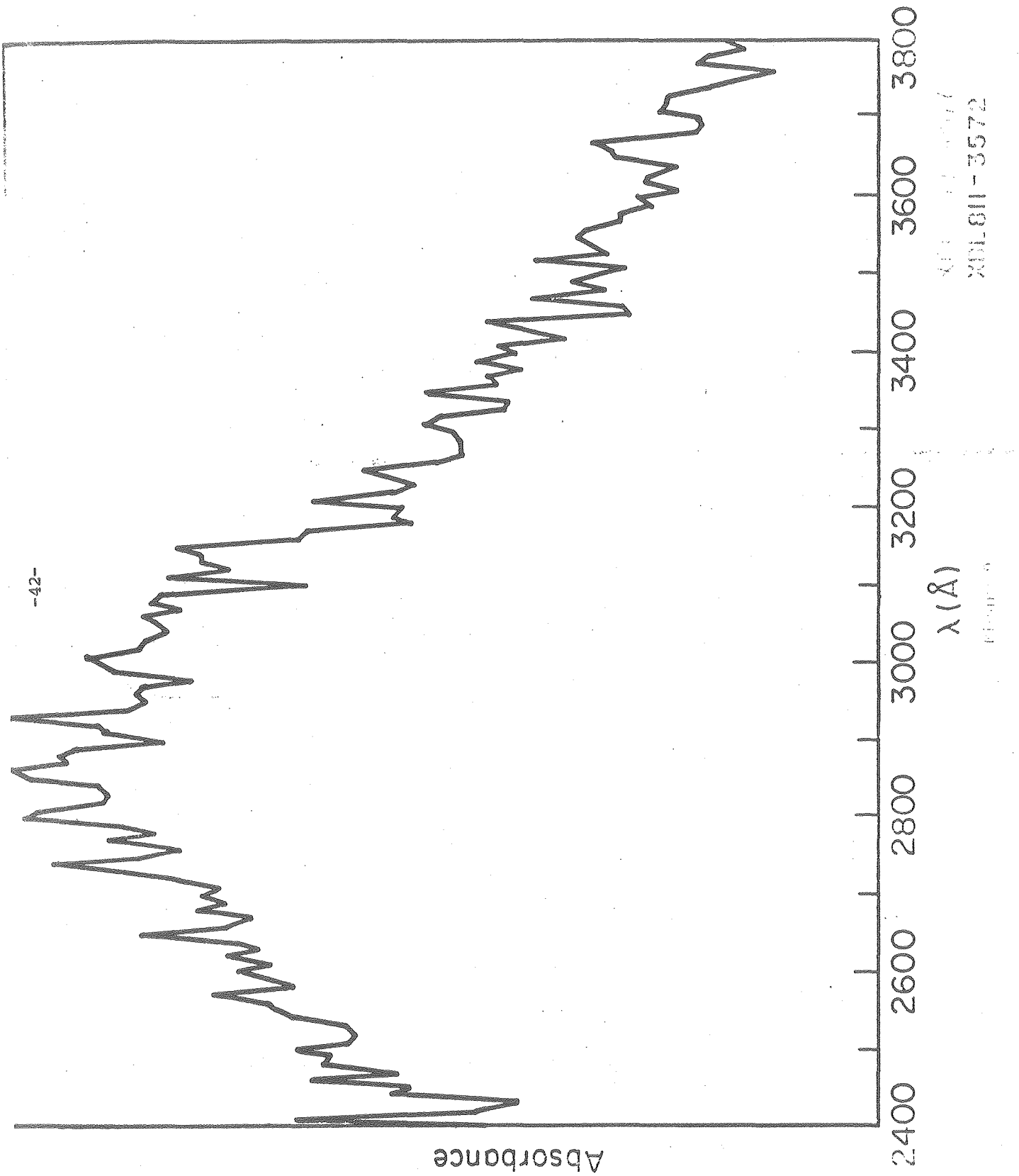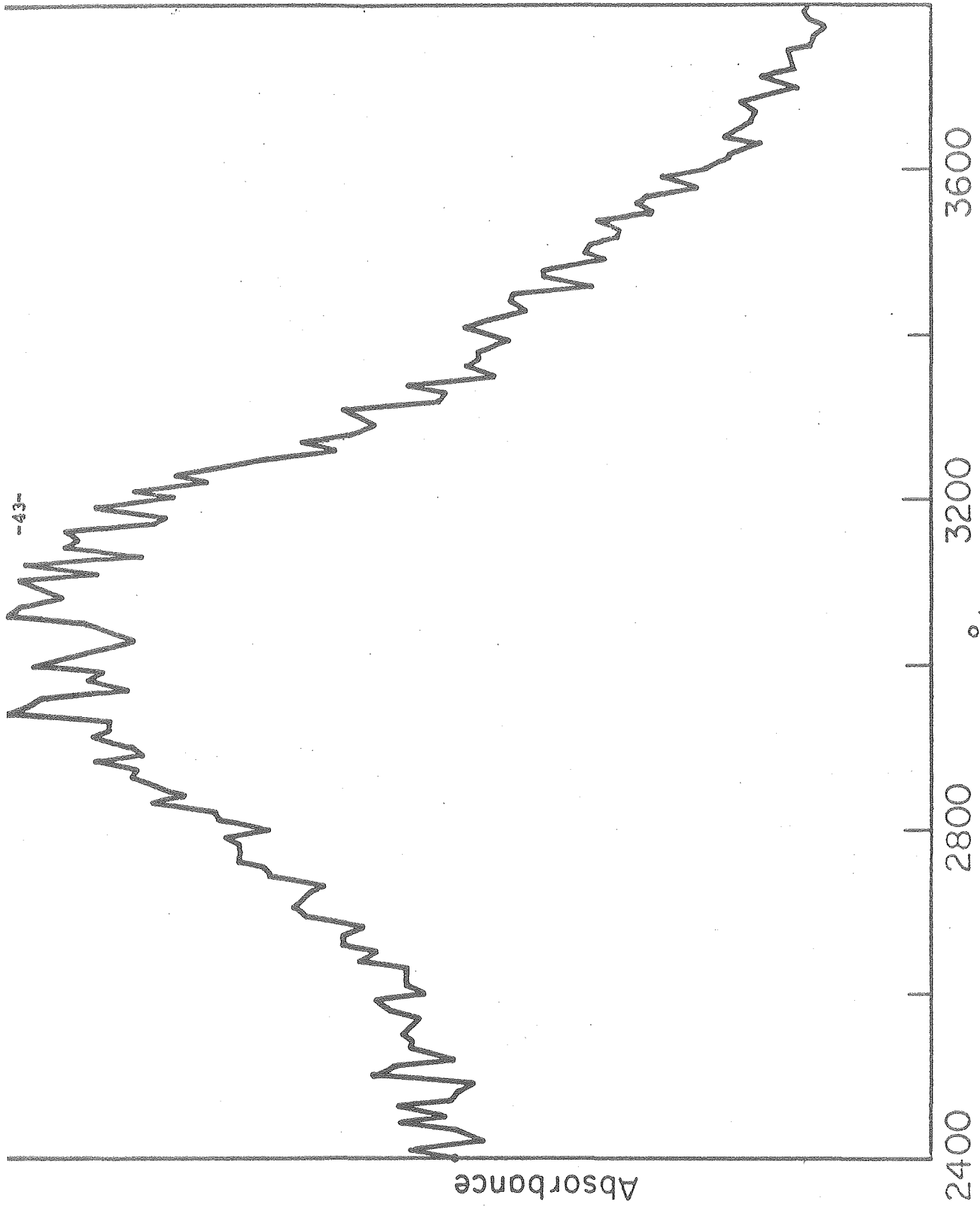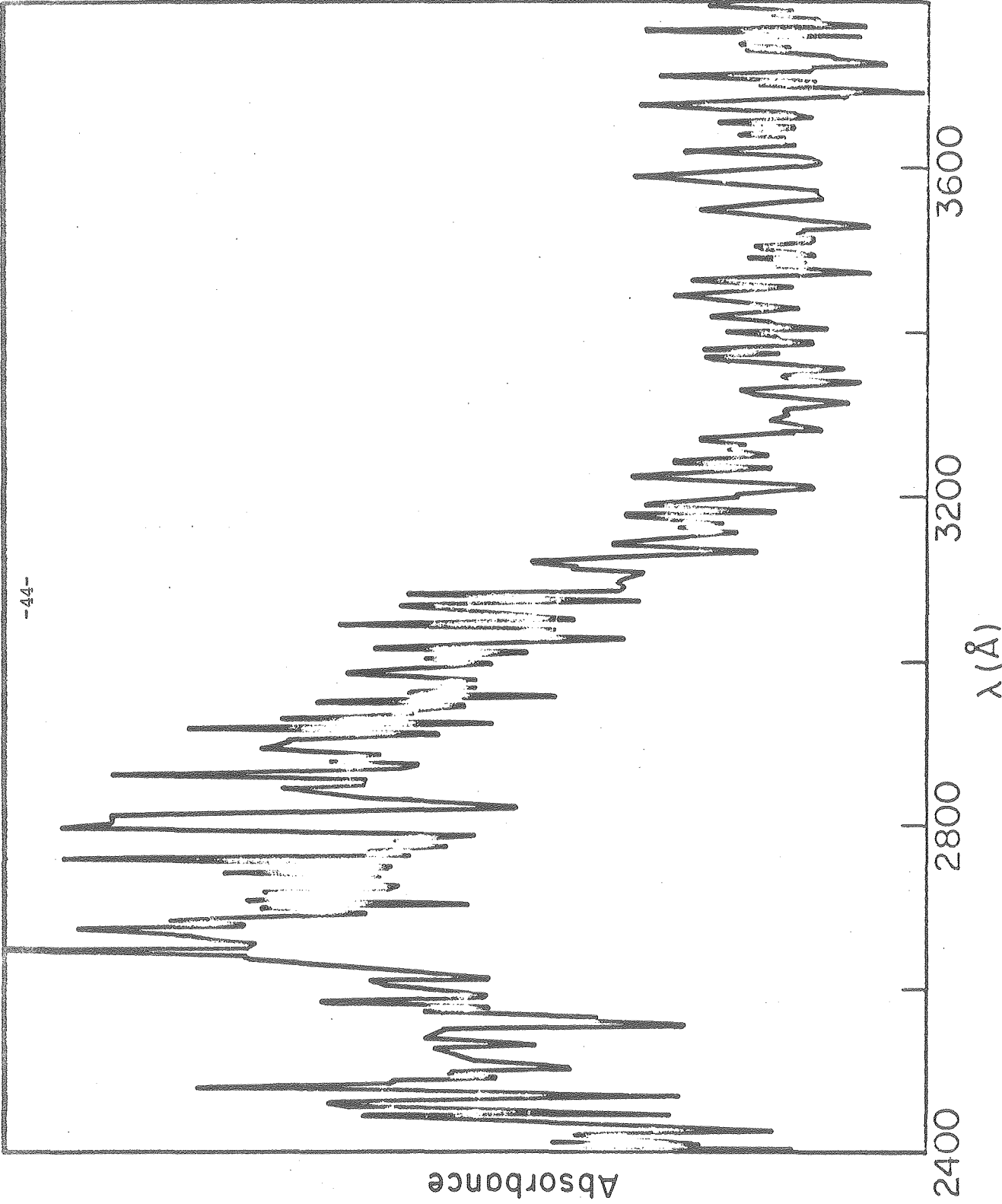
λ (Å)

Figure 7

2400   2800   3200   3600

-40-

-41-

Absorbance

λ(Å)

2400   2800   3200   3600

XBL811-3572

Figure 8

-42-

$\lambda (\text{Å})$

Absorbance

Figure 10

Absorbance

$\lambda\,(\text{Å})$

2400   2800   3300   3600

—44—

Figure 11

XD1-811-80771

Absorbance

λ (Å)

2400

2800

3200

3600

-45

Refractive index

Absorption coefficient

$\lambda\,(\mathring{A})$

-46-

-47-

Absorbance

$\lambda(\text{Å})$

Figure 14

XBL1811-3568
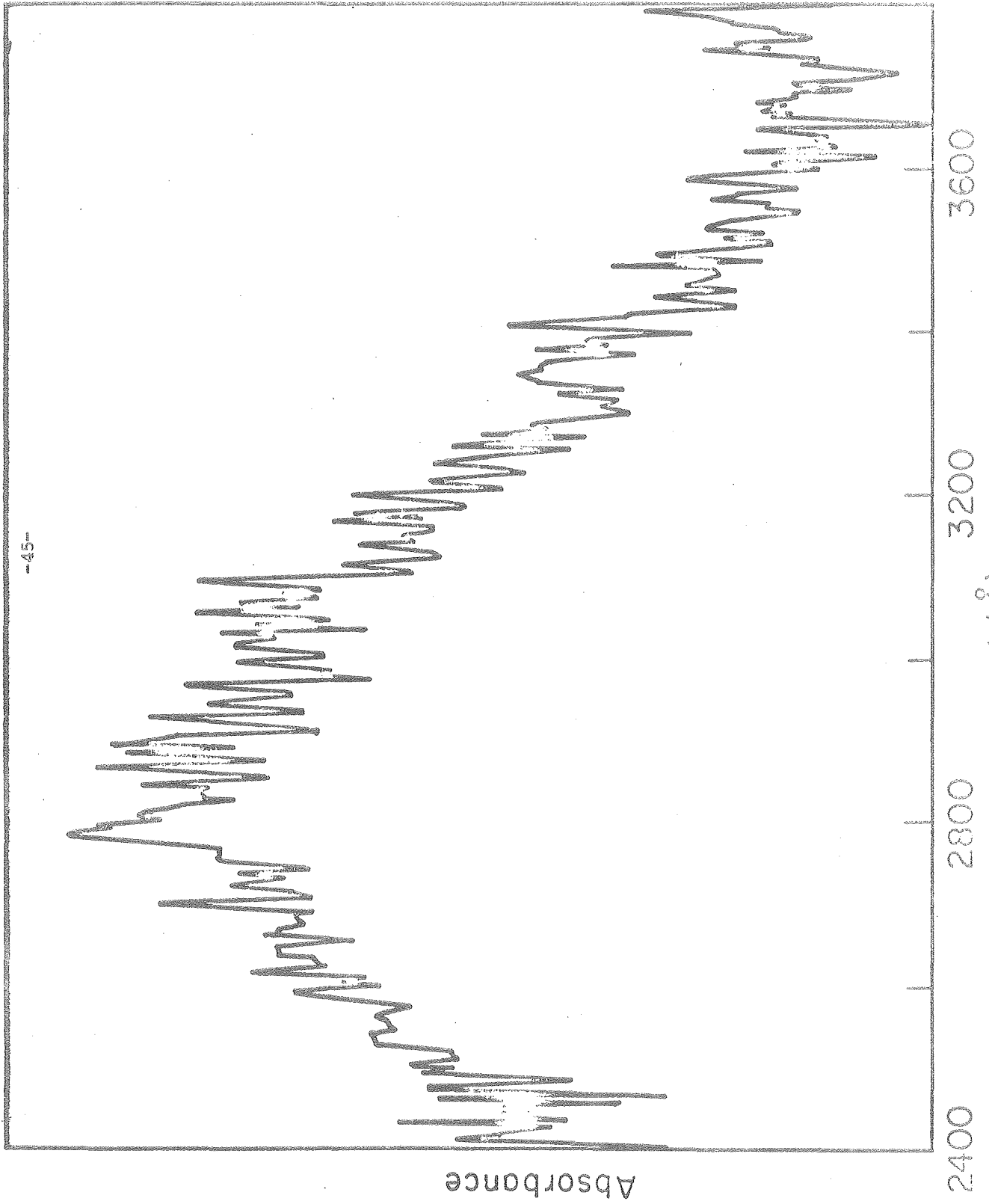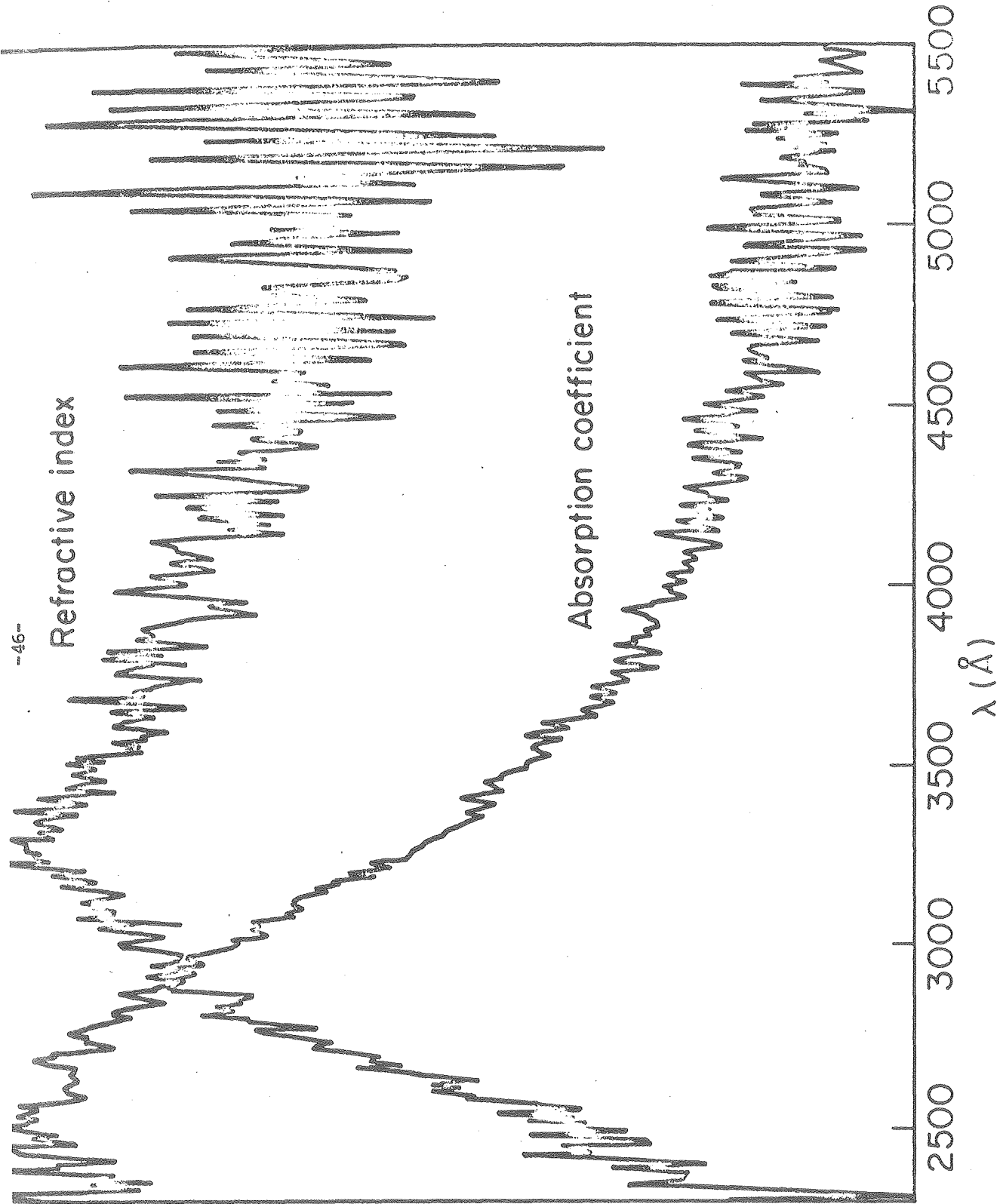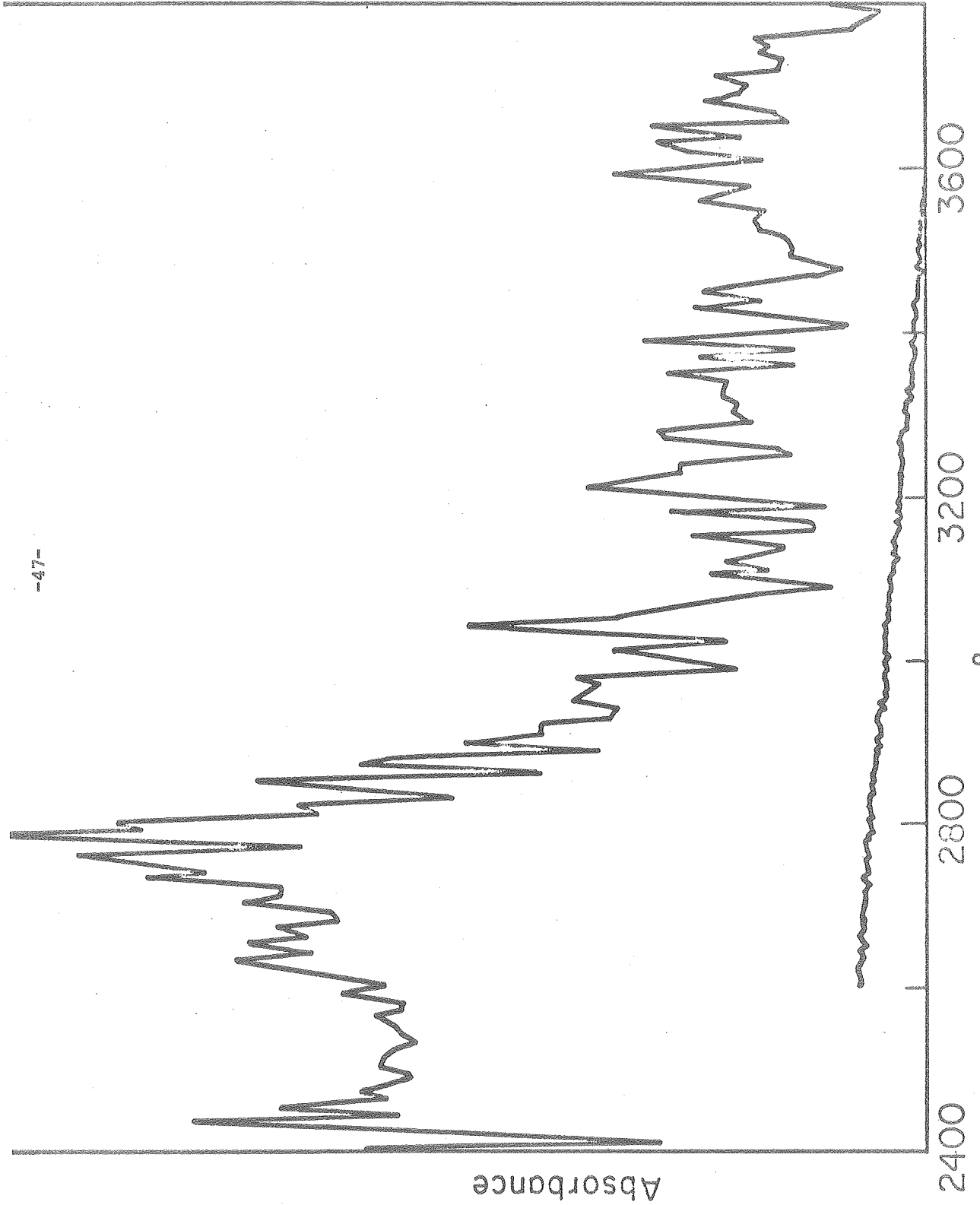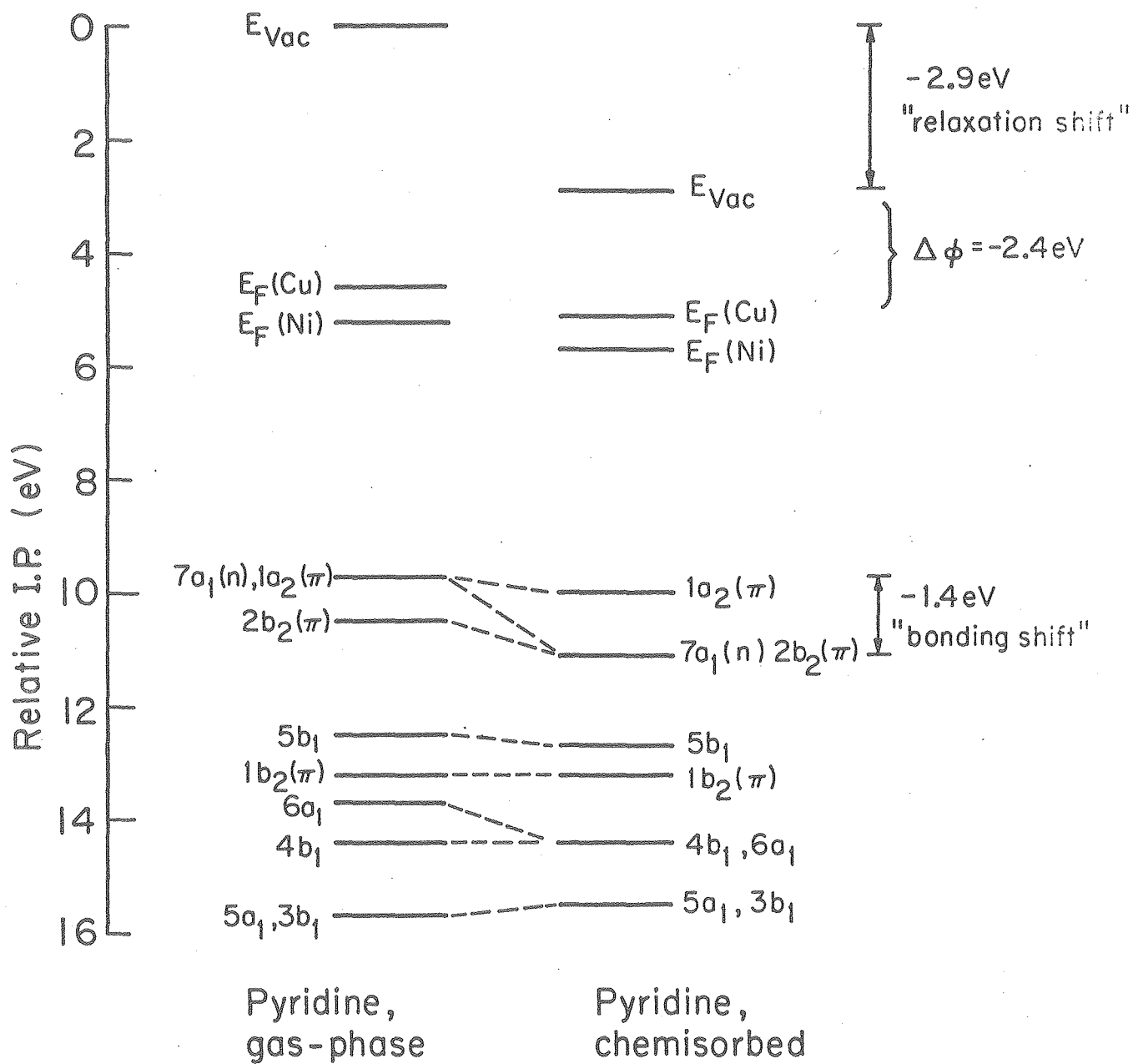
Figure 15

XBL811-3578
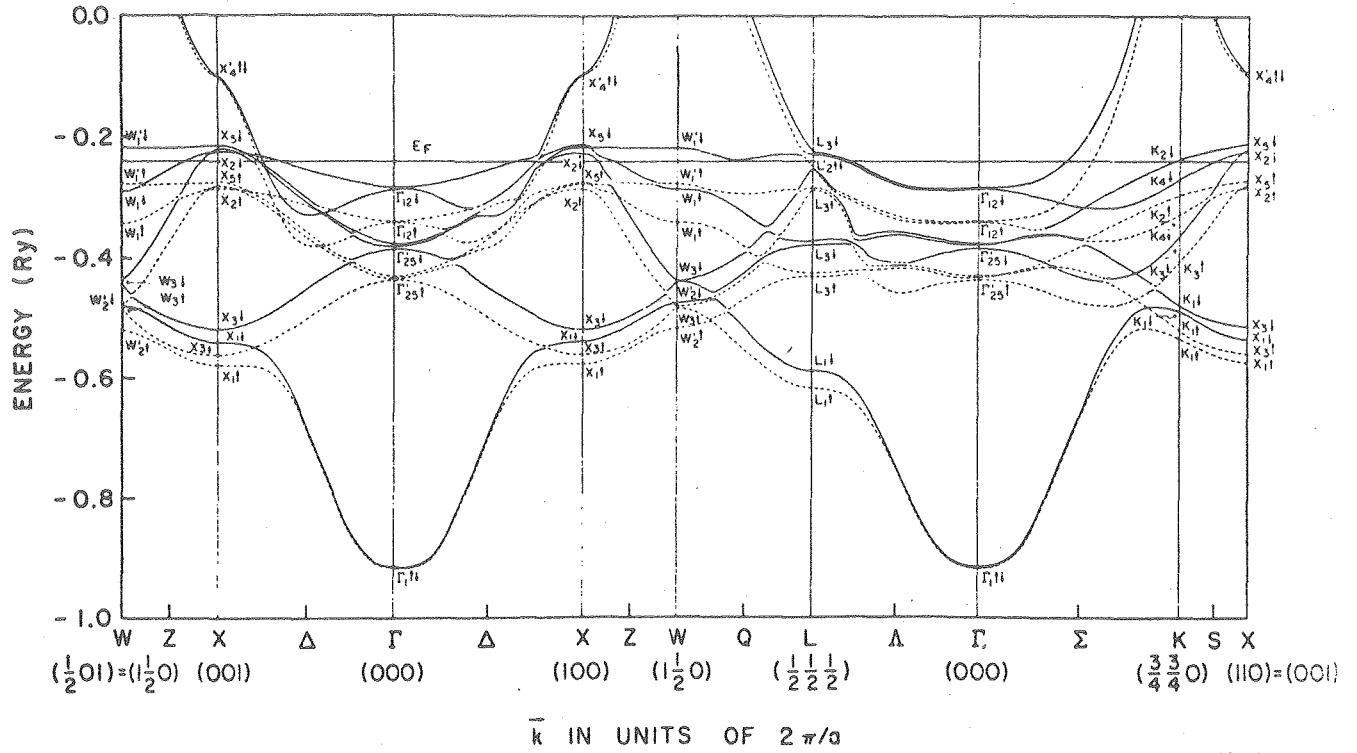
FIG. 1. Band structure of nickel along some symmetry lines in the Brillouin zone. States are labeled according to the symmetry of the largest spin component. The solid lines indicate states of minority spin, the dashed lines of majority spin.

Figure 16 a

Figure 16 b